Overview of a Carbon Steel Container Corrosion Model for a Deep Geological Repository in Sedimentary Rock

NWMO TR-2007-01 **March 2007**

Fraser King

Integrity Corrosion Consulting Limited

nwmo

NUCLEAR WASTE MANAGEMENT ORGANIZATION

SOCIÉTÉ DE GESTION DES DÉCHETS NUCLÉAIRES

Nuclear Waste Management Organization
22 St. Clair Avenue East, 6th Floor
Toronto, Ontario
M4T 2S3
Canada

Tel: 416-934-9814
Web: www.nwmo.ca

Overview of a Carbon Steel Container Corrosion Model for a Deep Geological Repository in Sedimentary Rock

NWMO TR-2007-01

March 2007

Fraser King
Integrity Corrosion Consulting Limited

Disclaimer:

This report does not necessarily reflect the views or position of the Nuclear Waste Management Organization, its directors, officers, employees and agents (the “NWMO”) and unless otherwise specifically stated, is made available to the public by the NWMO for information only. The contents of this report reflect the views of the author(s) who are solely responsible for the text and its conclusions as well as the accuracy of any data used in its creation. The NWMO does not make any warranty, express or implied, or assume any legal liability or responsibility for the accuracy, completeness, or usefulness of any information disclosed, or represent that the use of any information would not infringe privately owned rights. Any reference to a specific commercial product, process or service by trade name, trademark, manufacturer, or otherwise, does not constitute or imply its endorsement, recommendation, or preference by NWMO.

ABSTRACT

Title: **Overview of a Carbon Steel Container Corrosion Model for a Deep Geological Repository in Sedimentary Rock**
Report No.: **NWMO TR-2007-01**
Author(s): Fraser King
Company: Integrity Corrosion Consulting Limited
Date: March 2007

Abstract
A conceptual model for corrosion of a carbon steel (C-steel) used fuel container in a deep geological repository in sedimentary rock is described. The model takes into account various corrosion processes that might affect the container in the repository environment. Some processes, such as uniform corrosion and localized (pitting) attack, are specifically included in the conceptual model for the calculation of the used fuel container lifetime. Other processes, such as hydrogen-related effects, stress corrosion cracking, microbiologically influenced corrosion, preferential weld corrosion, and dry air oxidation are excluded from the conceptual model. This is based on the assumptions that either the environment will not support these processes or that these corrosion processes can be avoided by proper container design and fabrication procedures. The validity of these assumptions would still need to be demonstrated in the future through more-detailed engineering assessment, mathematical modelling, and experimental studies.

The extent of uniform corrosion should be assessed through a combination of (i) mass-balance arguments in the case of aerobic conditions, (ii) empirical corrosion rate data for the anaerobic phase, and (iii) a mechanistic mixed-potential model to provide support and justification for the calculations of the rate of wall loss. This combination of empirical calculations and mechanistic modelling provides a justifiable, robust prediction of the long-term uniform corrosion behaviour of a C-steel used fuel container.

Similarly, the effect of localized corrosion on the lifetime of C-steel containers should be assessed through a combination of empirical data and mechanistic modelling. Empirical data can be used to estimate the time-dependence of the degree of localization, whereas mechanistic modelling is used to justify these long-term predictions.

Preliminary C-steel corrosion assessments suggest that, based on a combination of uniform and pitting corrosion, the range of wall penetrations will be 9-34 mm after 10,000 years and 34-175 mm after 100,000 years. It is expected that a steel container would still have sufficient remaining wall thickness and mechanical strength to avoid container failure or through-wall penetration for a period of more than 10,000 years after it is placed in a repository in sedimentary rock. This analysis suggests, therefore, that C-steel containers can provide containment of used fuel for substantial periods of time in a deep geological repository in sedimentary rock.

TABLE OF CONTENTS

Page

ABSTRACT ..... **v**

1. INTRODUCTION **1**

2. REVIEW OF THE EVOLUTION OF THE REPOSITORY ENVIRONMENT **3**

3. CORROSION PROCESSES OF INTEREST **7**

3.1 UNIFORM CORROSION **7**
3.1.1 Corrosion Rates 7
3.1.2 Electrochemical Considerations 14
3.1.3 Gas Generation and Transport 18
3.2 LOCALIZED CORROSION **21**
3.2.1 Mechanisms of Localized (Pitting) Corrosion of C-steel UFC 22
3.2.2 Treatment of Initiation and Propagation 26
3.3 HYDROGEN EFFECTS **29**
3.3.1 Hydrogen Degradation Mechanisms in Carbon Steel 29
3.3.2 Treatment of Hydrogen Degradation Mechanisms 32
3.4 STRESS CORROSION CRACKING **34**
3.5 MICROBIOLOGICALLY INFLUENCED CORROSION **38**
3.6 CORROSION BEHAVIOUR OF WELDS **39**
3.7 OXIDATION OF CARBON STEEL **40**

4. QUALITATIVE DESCRIPTION OF CORROSION BEHAVIOUR OF CARBON STEEL USED FUEL CONTAINERS **41**

5. CARBON STEEL CONTAINER FAILURE MODEL **44**

5.1 TREATMENT OF CORROSION PROCESSES **44**
5.1.1 Uniform Corrosion 44
5.1.2 Localized (Pitting) Corrosion 45
5.1.3 Hydrogen Effects 45
5.1.4 Stress Corrosion Cracking 45
5.1.5 Microbiologically Influenced Corrosion 46
5.1.6 Welds 46
5.1.7 Oxidation 46
5.2 CONTAINER FAILURE **47**
5.2.1 Mechanical Overload 47
5.2.2 Time Dependence of Failure Aperture 47
5.2.3 Preliminary Lifetime Assessment 47

6. CONCLUSIONS **48**

ACKNOWLEDGEMENT **48**

REFERENCES **49**

LIST OF TABLES

Page

Table 1: Summary of Corrosion Rate Predictions for C-steel Used Fuel Containers 59

LIST OF FIGURES

Page

Figure 1: Conceptual Designs for the Long-term Management of Spent Nuclear Fuel or High-level Waste in C-steel Containers from Various International Programs 2
Figure 2: Evolution of Environmental Conditions in a Deep Geological Repository Characterized in Terms of the Stages of Saturation 6
Figure 3: Time Dependence of the Corrosion Rate of Carbon Steel in Compacted Bentonite and Bentonite Slurry Under Aerobic Conditions at 80°C 9
Figure 4: Dependence of the Corrosion Rate of Carbon Steel on Bentonite Dry Density Saturated with Aerated Solutions 9
Figure 5: Dependence of the Corrosion Rate of Carbon Steel on Chloride Concentration in Compacted Bentonite Under Aerobic Conditions 10
Figure 6: Temperature Dependence of the Corrosion Rate of Carbon Steel in Compacted Bentonite Saturated with Aerated Solution 10
Figure 7: Time Dependence of the Corrosion Rate of Cast Iron and Carbon Steel in Deaerated Granitic Groundwater Measured Using the Rate of Hydrogen Generation 12
Figure 8: Compilation of Corrosion Rates of Carbon Steel Under Anaerobic Conditions Measured Using the Rate of Hydrogen Generation 12
Figure 9: Compilation of Corrosion Rates of Carbon Steel Under Anaerobic Conditions Measured Using the Mass Loss 13
Figure 10: Corrosion Rates of Carbon Steel and Cast Iron from Archaeological Analogs 15
Figure 11: Time Dependence of the Corrosion Potential of a Millscale-Covered C-steel Electrode in CO_2-Containing Solution 18
Figure 12: Schematic of Gas Transport Mechanisms in Opalinus Clay 19
Figure 13: Gas Transport Capacity for Various Gas Transport Mechanisms in Opalinus Clay as a Function of the Total Pressure 20
Figure 14: Potential-pH Diagram for the Fe-H_2O System at 25°C 21
Figure 15: Proposed Mechanism for the Distribution of Anodic and Cathodic Reactions for Micro- and Large Droplets of Water 22
Figure 16: Anodic Polarization Curves for C-steel in Compacted 70:30 Bentonite:Sand Buffer Material 23
Figure 17: Dependence of Repassivation Potentials for the Pitting and Crevice Corrosion of Carbon Steel on pH 24
Figure 18: Illustration of Possible Spatial Locations for Anodic and Cathodic Reactions on a Film-covered C-steel Surface 25
Figure 19: Relationship Between the Pitting Factor and the Mean Corrosion Depth for Carbon Steel Exposed to Various Environmental Conditions 28
Figure 20: Schematic Illustrating the Zones of Susceptibility of Carbon Steel to Hydrogen-related Degradation Mechanisms Based on the Absorbed Hydrogen Concentration and the Material Yield Strength 30

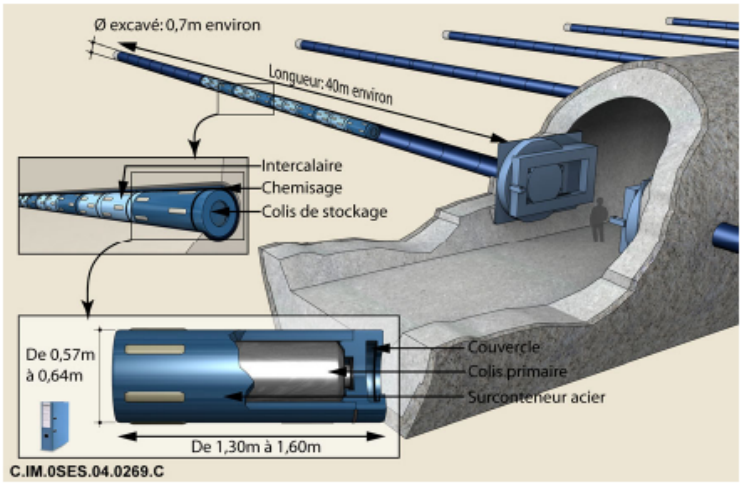
Figure 21: Effect of Various Environmental Parameters on the Sub-surface Absorbed Hydrogen Concentration 31
Figure 22: Potential-pH Diagram for Iron Showing the Regions of Susceptibility for the Two Forms of Stress Corrosion Cracking of C-steel Pipelines 35
Figure 23: Cross-section of Dormant Crack in Pipeline Steel 36
Figure 24: Effect of Shot Peening on the Distribution of Residual Stress on Pipeline Steels 37
Figure 25: Depth Dependence of the Residual Stress in the Hoop and Radial Directions for the Laser-Peened Outer Closure Lid and the Middle Closure Lid Welds for an Alloy 22 Waste Package 37
Figure 26: Schematic of Expected Evolution of the Corrosion Potential of a Carbon Steel Used Fuel Container in a Canadian Repository in Sedimentary Host Rock 41

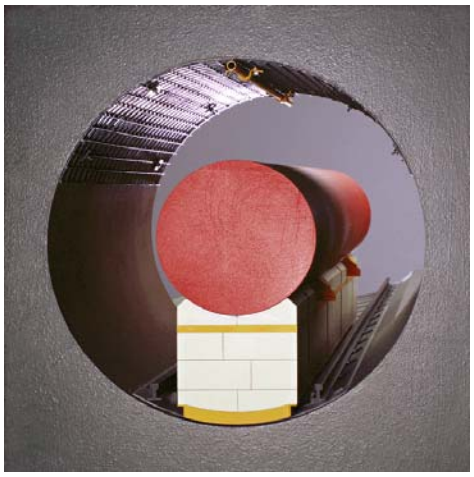
1. INTRODUCTION

The Nuclear Waste Management Organization (NWMO) is developing the technology for the management of Canada's nuclear fuel waste (NWMO 2005). One aspect of the NWMO's research and development program is advancing the technology associated with a deep geological repository (DGR) for used fuel in a suitable formation such as the crystalline rock of the Canadian Shield or Ordovician sedimentary rock (Gierszewski et al. 2004, Mazurek 2004). For the DGR concept, used fuel would be placed and isolated in corrosion-resistant containers in a stable host-rock formation (NWMO 2005, Russell and Simmons 2003). Copper is the current reference corrosion-barrier material for the used fuel container (UFC) (Maak 1999), although the use of carbon steel (C-steel) is also being considered (King 2005a). Although Cu containers are likely to have longer lifetimes than C-steel containers, the shorter-lived C-steel containers may provide adequate safety in deep, low-permeability sedimentary formations.

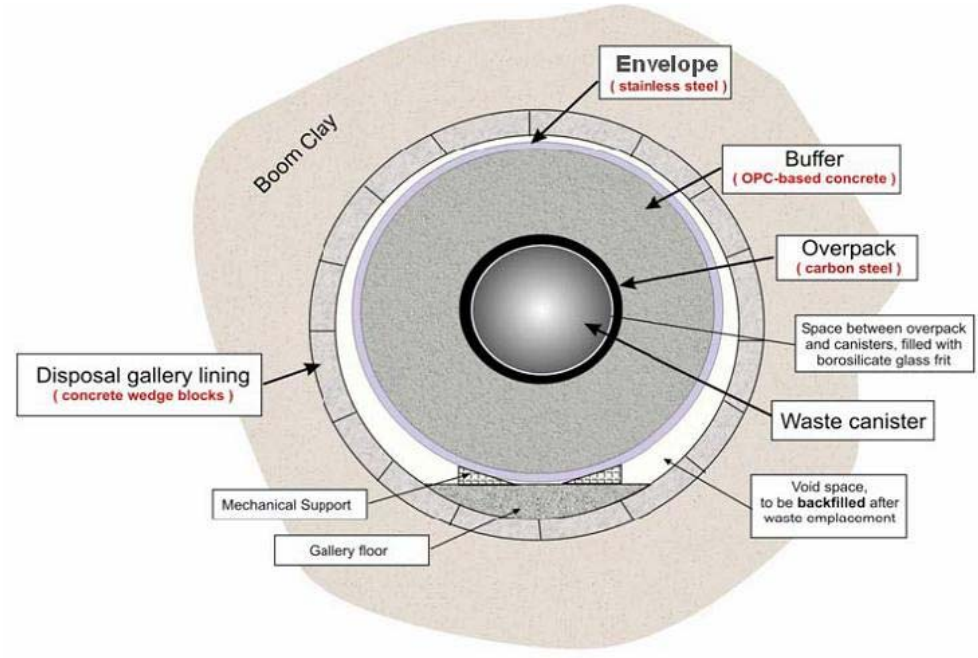
A number of countries have considered the use of C-steel containers in a variety of host rock formations. Of these different international programs, the most developed are those in France, Switzerland, and Belgium (Figure 1). France is considering the horizontal placement of C-steel canisters in boreholes in argillaceous clay (Figure 1(a)). The boreholes would not be backfilled to allow for retrieval for a period of up to 300 a. Environmental conditions are expected to result in uniform corrosion only (Andra 2005). Switzerland is considering the use of C-steel canisters for the placement of high-level waste and spent nuclear fuel in a backfilled deep geological repository in the sedimentary Opalinus Clay formation (Nagra 2002). The canisters would be placed on blocks of pre-compacted bentonite and the remaining void space filled with granular bentonite pellets (Figure 1(b)). Environmental conditions in the repository would closely resemble those expected in a DGR in sedimentary formations in Canada. Corrosion is expected to be primarily uniform in nature, with a small degree of localized attack (Johnson and King 2003). The Belgian program has recently re-designed its repository concept in favour of a supercontainer comprising a C-steel overpack encased in a cementitious buffer material surrounded by a stainless steel envelope (Bel et al. 2006). The supercontainers would be placed in horizontal boreholes in Boom clay sedimentary deposits. One of the major driving forces behind the re-design was the desire to create an alkaline near-field environment for improved corrosion resistance of the C-steel canister.

Other countries that have considered the use of a C-steel UFC include Japan, Germany, and the United Kingdom. Carbon steel is the reference container material in Japan (JNC 2000), but no host-rock formation has yet been selected. The generic program involves the placement of the high-level waste containers in a DGR and the backfilling of repository rooms with a bentonite-based material. Various container materials have been considered in the German program, with the focus on developing a deep geological repository in a salt formation (Smailos et al. 1985). Carbon steel was among those materials evaluated, but the program has not developed further over the past several years. The United Kingdom were also an early proponent of the use of C-steel, with a focus on a granitic host rock in the 1980's (Marsh and Taylor 1988). Recently, the U.K. high-level waste program has re-started but it is unclear at this stage whether C-steel will be the reference container material.





(a) France **(b) Switzerland**



(c) Belgium

Figure 1: Conceptual Designs for the Long-term Management of Spent Nuclear Fuel or High-level Waste in C-steel Containers from Various International Programs.

Since the use of C-steel was first proposed in the 1980's, much has been learnt of the corrosion behaviour under expected environmental conditions within a DGR. This increased understanding has lead to increased confidence in the use of C-steel for long-lived containers and a corresponding acceptance that container lifetimes could be substantially longer than the 1000-year period originally envisaged (Marsh and Taylor 1988, JNC 2000). Lifetimes as long as 10,000 years (Johnson and King 2003) or longer (King 2005a) are now being proposed for C-steel UFC.

An international consensus on the important corrosion processes for C-steel in a backfilled DGR is now emerging (JNC 2000, Johnson and King 2003, King 2005a). The container will be subject to uniform corrosion, which initially could take the form of uneven or localized attack. The degree of localization is expected to diminish with time. Hydrogen (H) produced by anaerobic corrosion will be absorbed by the container material, but proper selection of material should preclude effects such as hydrogen-induced cracking (HIC) or blistering. Similarly, stress corrosion cracking (SCC) and microbiologically influenced corrosion (MIC) can be ruled out based on proper container fabrication and repository design.

Here, the basis for a conceptual model for the corrosion of C-steel UFC in a DGR in sedimentary rock is presented. Detailed mathematical models and predictions of container lifetimes are not given. Rather, the focus is on the underlying mechanistic understanding underpinning the conceptual models. First, a brief review of environmental conditions in a possible DGR in sedimentary host rock is given, followed by a review of the relevant corrosion processes for C-steel. Based on this discussion, a qualitative description is then given of the expected corrosion behaviour of C-steel under the proposed repository conditions. Finally, the conceptual C-steel corrosion model is presented, along with a discussion of processes leading to ultimate failure of the container and preliminary lifetime predictions.

2. REVIEW OF THE EVOLUTION OF THE REPOSITORY ENVIRONMENT

One of the most important features of any deep geological repository is that the nature of the environment evolves over time. Generally, the environment evolves in such a way that corrosion becomes less severe and more predictable with time. The most aggressive forms of corrosion (e.g., localized corrosion, stress corrosion cracking) occur during the initial transient conditions. The long-term period is characterized by corrosion processes that result in slower and more predictable penetration, such as uniform corrosion. Here, the repository environment is discussed in terms of the following parameters: saturation of the repository, temperature, groundwater and pore-water chemistry, redox conditions, microbial activity, mass transport, residual stress and external loads, and gas transport mechanisms.

The repository sealing materials will be placed in an unsaturated condition. Depending upon the local hydraulic conductivity, saturation of the repository with groundwater could take 100's or 1000's of years. The degree of saturation is important in determining the availability of water (H_2O) to support electrochemical corrosion processes and the mass-transport of dissolved and gaseous species to and from the container surface. Initially, there will be insufficient moisture to support aqueous corrosion processes (King 2006). Only when the relative humidity increases, and the UFC surface temperature decreases, will deliquescence of salt deposits on the container surface occur and corrosion become possible. The supply of H_2O could be rate-limiting initially, especially for the corrosion of steel and the consequent production of hydrogen

gas (H_2). Eventually the repository will become saturated with water and corrosion will occur in a continuous water phase. In general, the dry-out phase will be longer (i) the drier the placed bentonite materials, (ii) the higher the maximum container surface temperature, and (iii) the lower the hydraulic conductivity of the host rock.

The maximum UFC surface temperature is a design parameter dependent on a number of factors, including the age and degree of cooling of the used fuel, the spacing of containers, the thermal conductivity of the sealing materials and their initial moisture content, the ambient host rock temperature, and the thermal conductivity of the sedimentary deposit. Historically, maximum UFC temperatures have been limited to ~100^{o}C to avoid alteration of the bentonite. However, the reference Swiss concept for a DGR in Opalinus clay involves a maximum temperature of 150-160^{o}C. The higher temperature is partly a result of a higher ambient temperature at repository depth and partly a result of the low initial moisture content of the bentonite sealing materials (Nagra 2002). The consequences of thermal alteration of the bentonite can be offset by using a thicker layer of bentonite, since only that portion of the bentonite closest to the UFC surface may be altered during the relatively short thermal pulse. However, the effect of bentonite alteration adjacent to the container on its ability to inhibit microbial activity on or near the container surface still needs to be assessed.

The bentonite pore-water will undergo significant chemical changes during the evolution of the repository environment. The initial composition will be determined by the nature of the water used to wet the dense bentonite (groundwater, potable water) and the content of soluble mineral impurities in the clay. Eventually, the pore water will equilibrate with the groundwater, which tends to be highly saline at the proposed depths for a repository in the Michigan Basin (40,000-300,000 mg·L^{-1} total dissolved solids, King 2005b).

King (2005b, 2006) has described a sequence of events in the evolution of the pore-water chemistry:

1. Dissolution of soluble mineral impurities (NaCl, $CaCl_2 \cdot xH_2O$, $CaCO_3$, $CaSO_4 \cdot 2H_2O$) in the water added for compaction of the sealing materials.
2. Ion exchange with the sodium bentonite, resulting in the uptake of Ca^{2+} and the release of Na^{+} ions.
3. Precipitation of the least soluble minerals as water is driven away from the container surface by the thermal gradient.
4. Control of the pore-water pH in the range pH ~7-8 by calcite precipitation/dissolution.
5. Re-dissolution of precipitated minerals as the sealing materials re-wet, starting with the most soluble (most deliquescent) phases.
6. Eventual saturation of the sealing materials.

For the present purposes, the long-term, equilibrated pore-water composition is defined as (King 2005b):

- 1.1 mol·dm^{-3} Na^{+}
- 0.5 mol·dm^{-3} Ca^{2+}
- 2.1 mol·dm^{-3} Cl^{-}
- 0.005 mol·dm^{-3} SO_4^{2-}

corresponding to a total dissolved solids content of ~120,000 mg·L^{-1}.

Currently, there is limited mineralogical information of the sedimentary formations at the possible repository horizon depth in Canada. Potential host formations in Belgium and Switzerland contain significant amounts of pyrite (Nagra 2002, ONDRAF-NIRAS 2002). Dissolution of pyrite could lead to sulphide diffusing to the container surface or, during the initial aerobic transient, intermediate oxidation products such as thiosulphate.

As widely understood, the redox conditions in the repository will evolve from an initial aerobic phase to a long-term stable anaerobic condition. The duration of the aerobic phase is currently unknown but, based on calculations performed for other repository designs in Canada and internationally, is likely to be of the order of a few 10's of years to a maximum of 100-200 years (see, for example, Kolar and King 1996). Oxygen will be consumed by corrosion of the container, aerobic microbial activity in regions of the repository not sealed using highly compacted bentonite, and the oxidation of Fe(II) and other oxidizable minerals. Deep geological repositories typically contain 1-10 $mol_{O2} \cdot m^{-2}$ of container surface area. If all of this oxygen (O_2) resulted in uniform corrosion of the container, the resulting wall loss would be of the order of 10-100 μm. Therefore, the container alone represents a massive inventory of reduced material which will ensure that anaerobic conditions are maintained in the repository indefinitely.

Much effort has been put into characterizing deep sub-surface microbes and the factors that control their activity (see, for example, King and Stroes-Gascoyne 1995, 1997; King et al. 2004; Motamedi 1999, Pedersen 2000, Pedersen et al. 2000, Stroes-Gascoyne and King 2002, Stroes-Gascoyne et al. 2006, 2007). There is now strong evidence that microbes will not survive and/or are inactive in highly compacted bentonite. The physiological reason is uncertain, but is thought to involve either the effect of compaction density on the availability of water or the high swelling pressures in saturated bentonite. Regardless, a bentonite dry density of $\geq$1.6 $Mg \cdot m^{-3}$ is sufficient to suppress all microbial activity. It is assumed here that the containers will be placed in compacted buffer material that meets or exceeds this required dry density, and that microbial activity close to the container surface will not occur at anytime during the lifetime of the UFC. However, it is accepted that microbial activity may occur in other regions of the repository not sealed with highly compacted bentonite. Under these circumstances, aggressive metabolic by-products could diffuse to the container surface.

One of the purposes for sealing the repository with highly compacted bentonite is to limit the rate of mass transport of species to and from the container. In saturated bentonite, mass transport occurs by diffusion only, at a rate approximately two orders of magnitude slower than in bulk solution (King et al. 1996). In unsaturated bentonite, however, the diffusivity of dissolved species is diminished and the diffusivity of gaseous species enhanced (King 2006).

The magnitude of the load acting on the container shell will determine its structural integrity. The UFC is required to withstand external loads resulting from (i) the swelling pressure exerted by the bentonite (2-4 MPa), (ii) the volume expansion of C-steel corrosion products, (iii) the hydrostatic load (for example, 6 MPa at a depth of 600 m), (iv) the lithostatic load, (v) the development of a gaseous H_2 phase due to the anoxic corrosion of steel (maximum pressure 8-10 MPa, King 2005b), and (vi) additional hydrostatic and lithostatic loads from future glaciation events. In addition, residual stresses from container fabrication, especially the final closure weld, will be present, although may be offset to some degree by non-thermal post-weld stress relief. This complex set of residual stress and external loading could induce stress-assisted failure mechanisms, such as stress corrosion cracking (SCC) or mechanical overload.

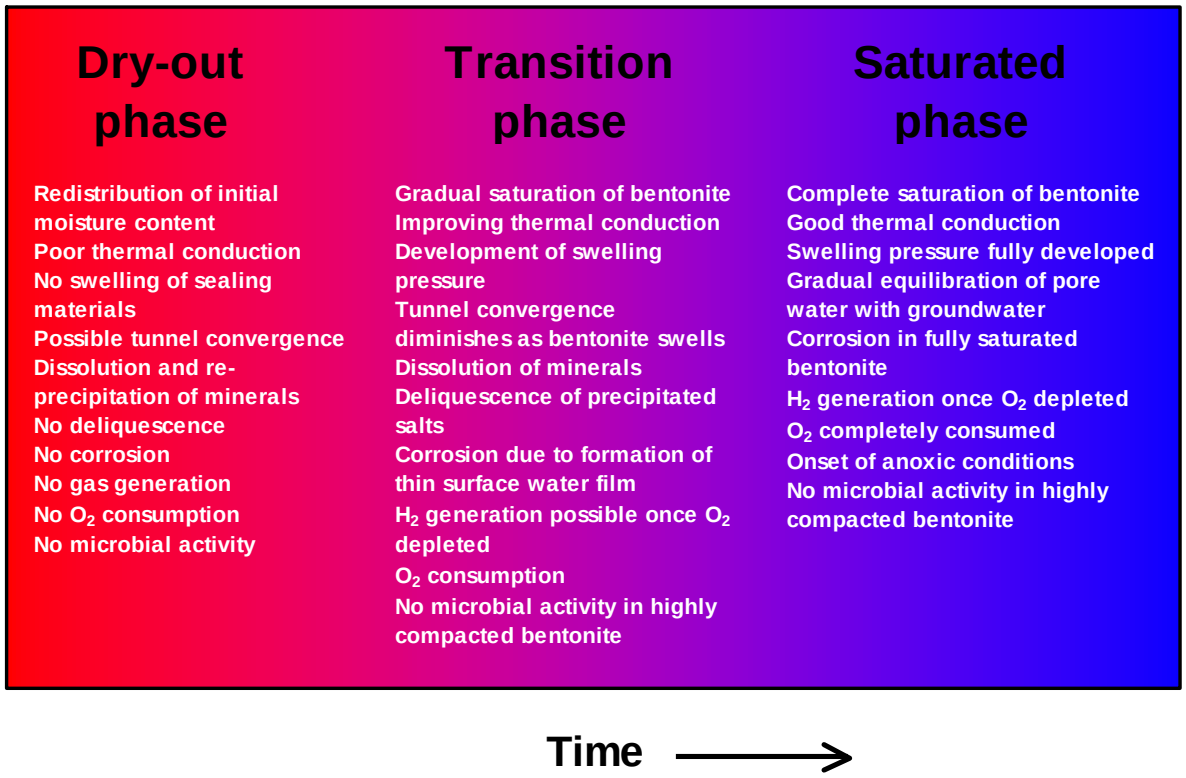


Figure 2: Evolution of Environmental Conditions in a Deep Geological Repository Characterized in Terms of the Stages of Saturation (King 2005b).

Hydrogen gas produced by corrosion of the UFC is unlikely to be removed from the repository by diffusion sufficiently fast to avoid the formation of a separate H_2 gas phase. Transport mechanisms for H_2 in low-permeability media are discussed in more detail in Section 3.1.3.

King (2005b) has characterized the evolution of the environmental conditions within a DGR in sedimentary rock in terms of different phases of saturation (Figure 2). This description is particularly apt for low-permeability host rocks as the rate of repository saturation is likely to be slower than in more-permeable fractured crystalline rock. The various processes that characterize the initial dry-out phase, the intermediate transition phase, and the long-term saturated phase are described in the figure. Superimposed on this variation in repository saturation is the transition from the initial warm, oxidizing environment to the long-term stable saturated anaerobic condition.

3. CORROSION PROCESSES OF INTEREST

Various corrosion processes of interest are discussed in this section, both processes that might lead to container failure and processes that can be excluded on the basis of UFC or repository design.

3.1 UNIFORM CORROSION

Carbon steel will undergo uniform, or general, corrosion in the repository environment. Uniform corrosion is usually discussed in either electrochemical terms (see Section 3.1.2) or in terms of measured corrosion rates (Section 3.1.1), typically measured by mass loss or, in the case of the anaerobic corrosion of C-steel, by the rate of H_2 generation. The rate of corrosion generally decreases with time either because of the depletion of reactants or, more usually, because of the formation of a protective corrosion product film.

3.1.1 Corrosion Rates

Given the expected evolution of the repository environment described above, C-steel containers will be subject to uniform corrosion under the following conditions:

1. Aerobic, unsaturated vapour phase
2. Aerobic, saturated aqueous phase or an anaerobic, unsaturated vapour phase
3. Anaerobic, saturated aqueous phase

Since O_2 consumption and water saturation are occurring simultaneously, the nature of the transitional period between the initial aerobic, saturated phase and the stable long-term anaerobic, saturated conditions is currently uncertain. If O_2 consumption is faster than the rate of saturation, then the transitional phase will involve a period of anaerobic, unsaturated conditions. If, however, water saturation is fast, the transitional phase will be characterized by a period of saturated, aerobic conditions. Both possibilities are considered here.

A compilation of reported corrosion rates from various nuclear waste management studies is given by King and Stroes-Gascoyne (2000).

<u>Aerobic, unsaturated vapour phase corrosion</u>

Aqueous corrosion of a C-steel UFC will first start when the container surface becomes wetted following the peak in the thermal pulse. Wetting of the surface will involve deliquescence of (i.e., the absorption of moisture by) surface contaminants in exactly the same manner as described for a Cu container by King (2006). Initial wetting of the surface is likely to lead to non-uniform corrosion, and will be discussed in more detail in Section 3.2. Corrosion will become more uniform once the surface becomes evenly wetted and there is no driving force for the spatial separation of anodic and cathodic sites.

On the assumption that the surface evenly wets prior to the consumption of O_2, there will be a period of aerobic corrosion of the C-steel container in partially saturated bentonite. Corrosion will be supported by the rapid diffusion of O_2 through the unsaturated bentonite (King 2006).

Relatively few corrosion studies have been performed under environmental conditions relevant to this period. Standard texts give ranges of corrosion rates for C-steel in different atmospheres at ambient temperature, with rates varying from ~10 $\mu m \cdot a^{-1}$ in urban and rural environments to ~100 $\mu m \cdot a^{-1}$ in marine locations (ASM 1987, Dechema 1990).

Studies in aerobic humid atmospheres for the Belgium program have resulted in a wide range of reported corrosion rates. In experiments in humid clay atmospheres at 170°C, Debruyn (1990) reported a rate of ~150$\mu m \cdot a^{-1}$, although in later reports the range of corrosion rates for as-received, heat-treated, and welded specimens was of the order of 0.02-2 $\mu m \cdot a^{-1}$ (Debruyn et al. 1991).

No other studies under repository conditions in humid aerobic atmospheres have been reported (King and Stroes-Gascoyne 2000).

Aerobic, saturated aqueous phase corrosion

A large number of C-steel corrosion studies have been performed in O_2-containing groundwater and compacted bentonite systems (King 2005a, King and Stroes-Gascoyne 2000). Solution compositions have ranged from dilute sedimentary and volcanic groundwaters to saline solutions simulating pore-fluids in salt deposits. Temperatures from ambient to 200°C have been used with exposure times up to 2-3 years, and over a pH range of pH 5-12.6. Given this wide range of environmental conditions and equally wide range of experimental techniques employed, it is not surprising that the reported corrosion rates also exhibit a wide range of values, from 2 to 2000 $\mu m \cdot a^{-1}$ (King 2005a, King and Stroes-Gascoyne 2000).

Rather than trying to derive an appropriate range of corrosion rates from these various studies, the discussion below focuses on one experimental study performed under well-controlled conditions. Honda et al. (1991) determined the corrosion rate of C-steel exposed to compacted bentonite under aerobic conditions for a range of conditions, including varying bentonite density, pore-water salinity, and temperature (Figures 3-6).

Mass transport and, to some degree, salinity, clearly have an effect on the corrosion rate of C-steel in aerobic compacted bentonite (Figures 3-5). More-restrictive mass transport, either through the used of compacted bentonite as opposed to a bentonite slurry (Figure 3) or through increasing the density of compacted clay (Figure 4), results in a decrease in corrosion rate due to transport limitation of the cathodic reduction of O_2. Corrosion rates are also higher in synthetic seawater (~0.5 $mol \cdot dm^{-3}$) than in distilled water, although the corrosion rate appears to be independent of salinity at higher Cl^- concentrations (Figure 5).

Corrosion rates also increase with temperature, albeit the dependence is fairly weak (Figure 6). Based on the data in Figure 6, the activation energy for the corrosion rate of C-steel in aerobic compacted bentonite is 1.3 $kJ \cdot mol^{-1}$ and 3.6 $kJ \cdot mol^{-1}$ for synthetic seawater and distilled water, respectively. These values are smaller than would be expected based on a diffusion-limited corrosion process (typically ~15 $kJ \cdot mol^{-1}$ in aqueous solution) or an activation-controlled process (typically 60 $kJ \cdot mol^{-1}$). The observed activation energy, however, is consistent with rate control by O_2 diffusion because the rate of supply of O_2 is determined by both the diffusivity, which increases with temperature, and the O_2 concentration, which decreases with temperature.

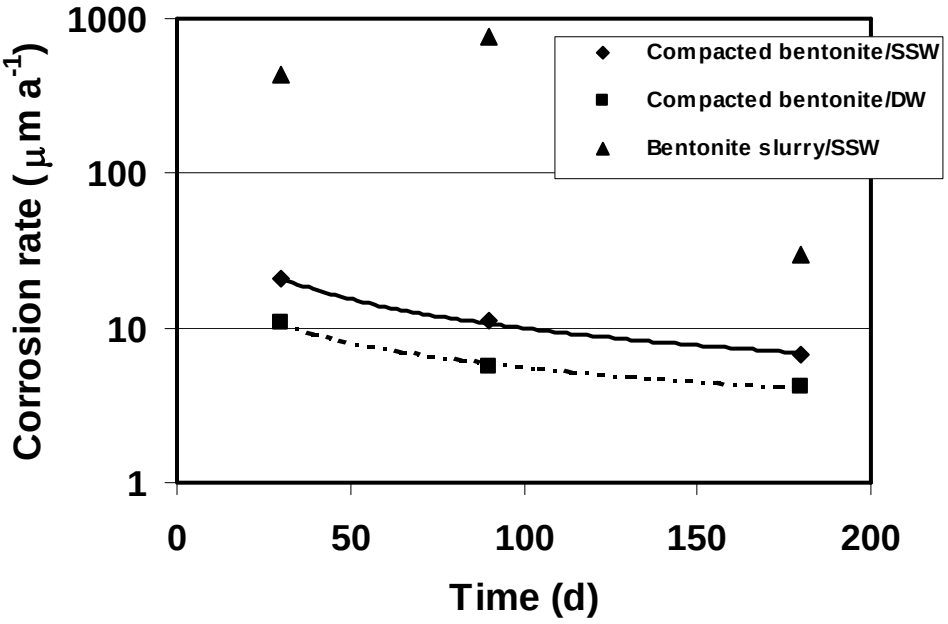


Figure 3: Time Dependence of the Corrosion Rate of Carbon Steel in Compacted Bentonite and Bentonite Slurry Under Aerobic Conditions at 80°C (after Honda et al. 1991). Bentonite compacted to a dry density of 1.32 Mg·m^{-3}. SSW – synthetic seawater, DW – distilled water.

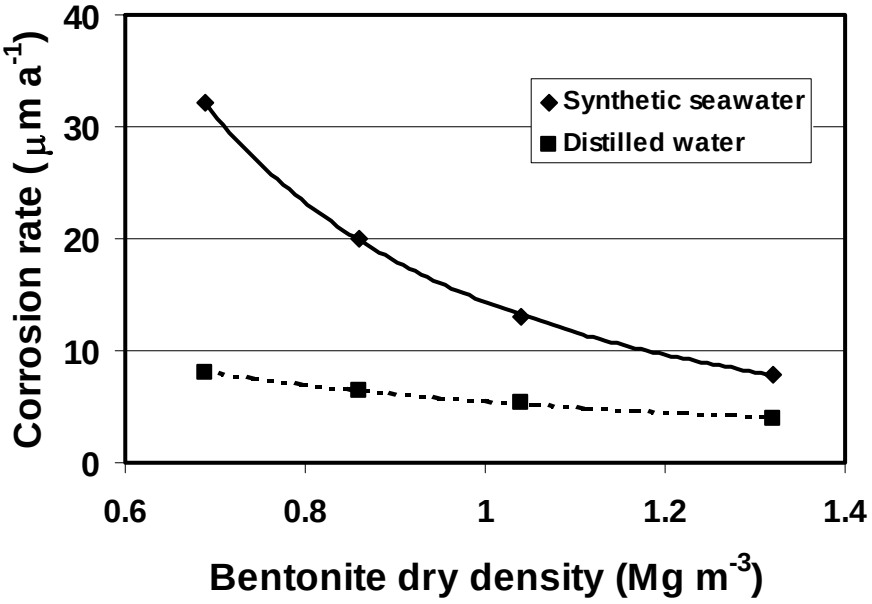


Figure 4: Dependence of the Corrosion Rate of Carbon Steel on Bentonite Dry Density Saturated with Aerated Solutions (after Honda et al. 1991). Exposure period of 180 d at a temperature of 80°C.

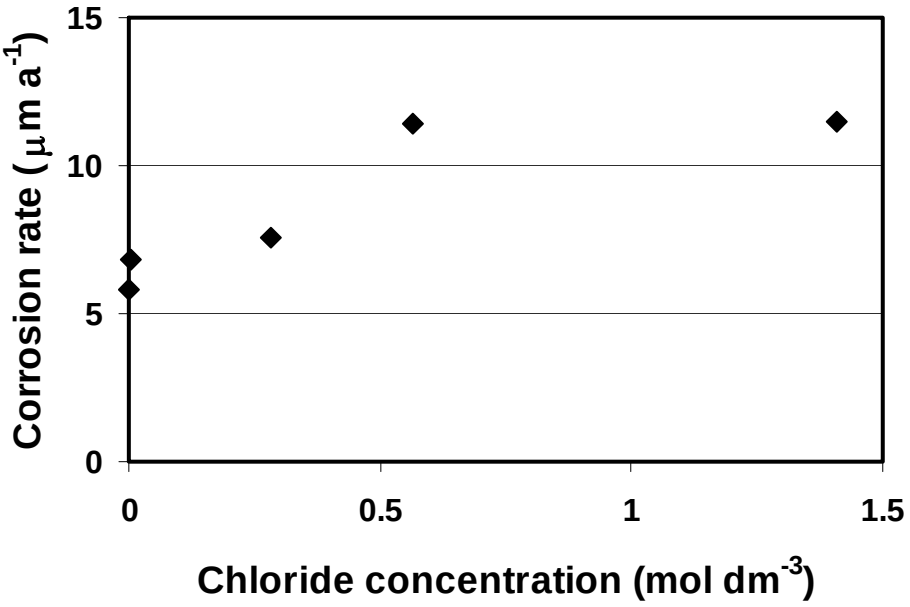


Figure 5: Dependence of the Corrosion Rate of Carbon Steel on Chloride Concentration in Compacted Bentonite Under Aerobic Conditions (after Honda et al. 1991). Bentonite dry density of 1.32 Mg·m^{-3} for an exposure period of 90 d at 80°C.

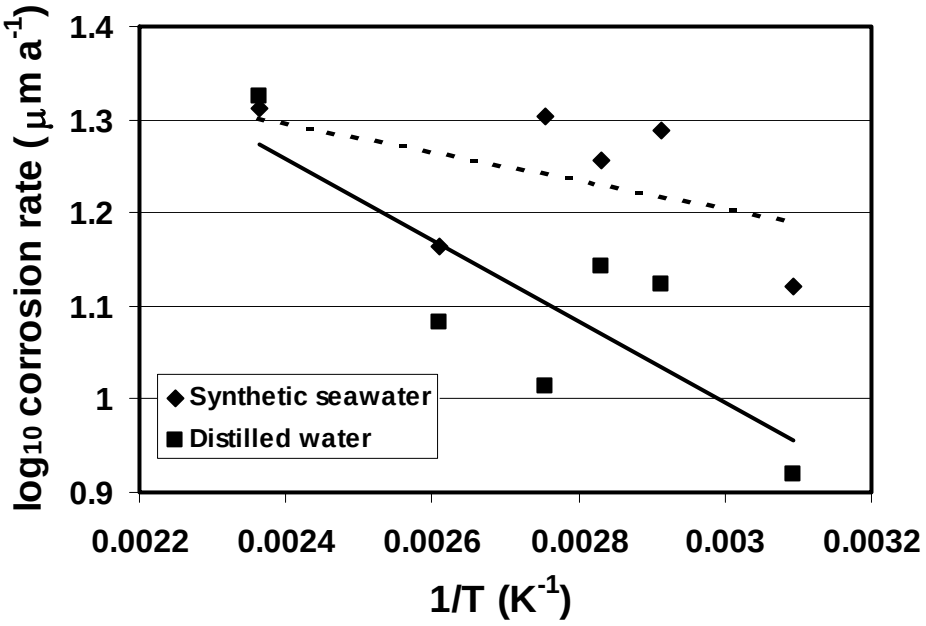


Figure 6: Temperature Dependence of the Corrosion Rate of Carbon Steel in Compacted Bentonite Saturated with Aerated Solution (after Honda et al. 1991). Bentonite dry density 1.32 Mg·m^{-3} for an exposure period of 90 d.

The Honda et al. (1991) study provides useful mechanistic information regarding the corrosion of C-steel in saturated compacted bentonite under aerobic conditions.

Anaerobic, unsaturated vapour phase corrosion

There are no reported studies of the corrosion of C-steel under anaerobic, unsaturated conditions in the nuclear waste management literature (King 2005a, King and Stroes-Gascoyne 2000). Furthermore, no studies in the general corrosion literature could be found under these conditions either. The reason for this lack of information is the fact that anaerobic vapour phase environments are not generally encountered. In addition, corrosion would not be expected to be severe under these conditions as there is no driving force for the spatial separation of anodic and cathodic processes, so that any corrosion that does occur would be in the form of slow uniform corrosion.

In the absence of specific corrosion rate measurements under these conditions, it is only possible to infer the likely corrosion behaviour based on the known mechanism of atmospheric corrosion. Corrosion in humid conditions occurs in a thin surface moisture film that forms on the surface due to the condensation of water vapour. Water condensation may be driven by the deliquescence of surface impurities or by condensation in pores and other surface discontinuities.

Typically, condensation of sufficient moisture to support electrochemical reactions occurs at 60-70% relative humidity (RH) (Shreir 1976). Although there is sufficient water present to enable corrosion to occur, there is a greater propensity for precipitation of corrosion products than in bulk solution because of the limited volume of water. Therefore, the corrosion rate is likely to be lower than in saturated systems where more dissolution would have to occur before the aqueous phase becomes saturated by, for example, $Fe(II)_{AQ.}$

Depending on the relative rates of corrosion and water saturation, it is possible that the corrosion rate could be limited by the supply of H_2O. Under anaerobic conditions, water acts not only as the electrolyte but also as the oxidant. If the supply of H_2O was rate limiting, then the thin moisture film would gradually dry out and electrochemical reactions cease until such time that the RH increases sufficiently to cause further surface wetting.

Anaerobic, saturated aqueous phase corrosion

In contrast, there are a large number of corrosion studies under anaerobic conditions in saturated systems (King 2005a, King and Stroes-Gascoyne 2000). Johnson and King (2003) have critically reviewed these studies and summarized the most pertinent corrosion rates (Figures 7-9). Figure 7 shows typical behaviour observed during laboratory testing, with the corrosion rate decreasing with time due to the formation of a protective corrosion product film. In the case of cast iron and C-steel, Smart et al. (2002) have reported a duplex magnetite (Fe_3O_4) film comprising an inner adherent layer formed by a solid-state process and a thicker outer layer formed by dissolution-precipitation.

There are two major questions to be answered when considering the long-term rate of anaerobic corrosion; first, what is the rate and, second, is the rate constant? The long-term corrosion rate can be estimated from the data compiled by King and Stroes-Gascoyne (2000). Depending upon the data considered, the long-term corrosion rate is of the order of

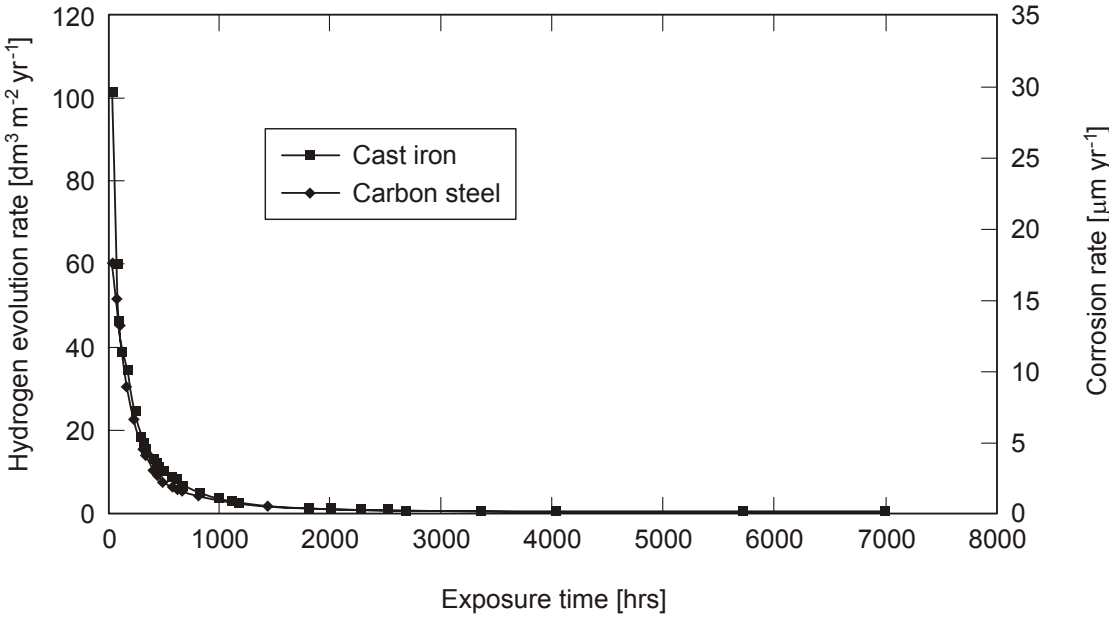


Figure 7: Time Dependence of the Corrosion Rate of Cast Iron and Carbon Steel in Deaerated Granitic Groundwater Measured Using the Rate of Hydrogen Generation (Smart et al. 2001, 2002).

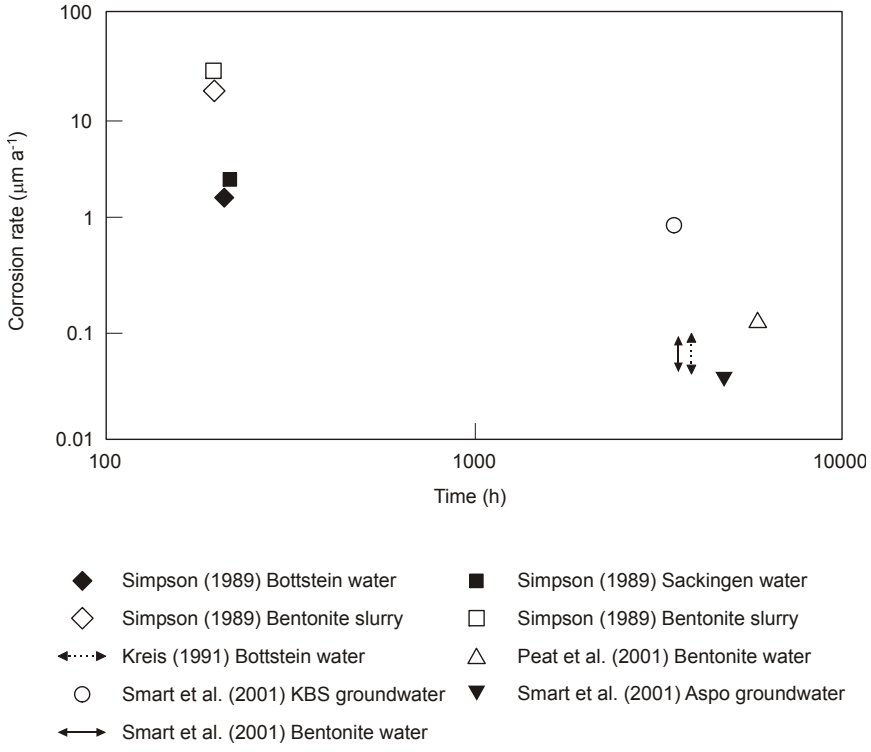


Figure 8: Compilation of Corrosion Rates of Carbon Steel Under Anaerobic Conditions Measured Using the Rate of Hydrogen Generation (Johnson and King 2003).

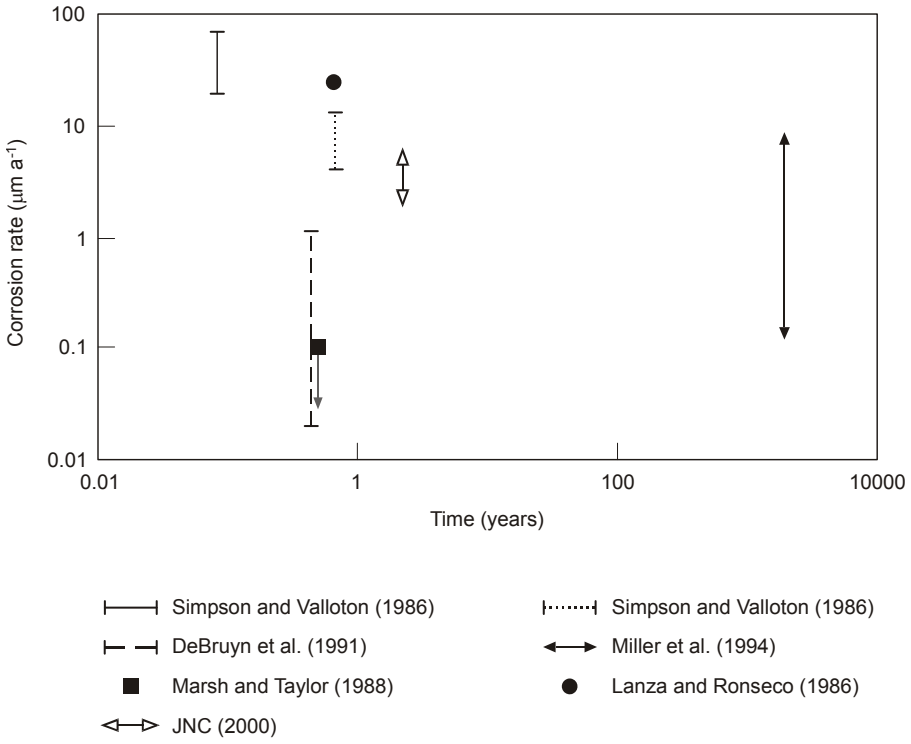


Figure 9: Compilation of Corrosion Rates of Carbon Steel Under Anaerobic Conditions Measured Using the Mass Loss (Johnson and King 2003).

0.1-10 $\mu m \cdot a^{-1}$ (Figures 8 and 9). Some of this variability is the result of environmental differences between the different studies, but some is also undoubtedly due to variability in the protectiveness of the corrosion product film. In turn, the protectiveness of the film depends on a large number of factors, including: the rate of precipitation, the solution pH, the extent to which groundwater species are incorporated into the film, the surface conditions and surface preparation method, temperature, etc. It is inherently difficult, therefore, to define a single "corrosion rate" and instead a range or distribution of rates is more appropriate.

The data in Figures 7-9 exhibit a tendency to reach a constant corrosion rate with increasing time (note that the logarithmic time scale in Figures 8 and 9 tend to obscure this trend). The mechanism of the anaerobic corrosion of C-steel is uncertain at this time, in particular the identification of the rate-determining process. If the surface is protected by a duplex Fe_3O_4 layer, as suggested by Smart et al. (2002), and if the rate of supply of H_2O is not rate limiting under saturated conditions, a constant corrosion rate could indicate that the film reaches a steady-state thickness and a constant porosity. Rate control might then be the dissolution of the Fe_3O_4 layer at the film/solution interface. However, typical values of the corrosion potential (E_{CORR}) under anaerobic conditions are not consistent with the equilibrium potential for Fe_3O_4/Fe(II) for reasonable concentrations of dissolved Fe(II). Alternatively, the corrosion rate could be limited by transport across the inner epitaxial layer (if such exists, as proposed by Smart et al. (2002)), either of Fe^{2+} or O^{2-} ions. It is also possible that transport of dissolved Fe(II) in the pores of the outer precipitated Fe_3O_4 film could be rate-determining. In this latter case, a constant film porosity and thickness would be required to explain the observed constant corrosion rate. Constant porosity could be maintained by the hydrolysis of Fe(II) within the

pores and the generation of acidity to prevent Fe_3O_4 precipitation, except at the film/solution interface. A constant film thickness could be produced by the periodic spalling of the film once it reached a critical thickness. At this stage, however, these mechanisms are somewhat speculative and a more-thorough analysis is required in order to support the use of a constant corrosion rate in C-steel UFC lifetime predictions.

Further evidence for the long-term corrosion rate of C-steel can be obtained from analog studies. Figure 9 shows the spread of corrosion rates (0.1-10 $\mu m \cdot a^{-1}$) derived from one such study (Miller et al. 1994). Additional long-term corrosion rates were discussed by Crossland (2005) and are presented in Figure 10. Data are presented for both soil environments and for artifacts exposed to bulk aqueous solution. The original author divided the data into aerobic and anaerobic environments in an arbitrary manner by drawing parallel lines through the data, the slopes of which represent the time dependence of the corrosion rate. Long-term (i.e., 100 a) anaerobic corrosion rates are of the order of 0.02-0.2 $\mu m \cdot a^{-1}$ in soil and 0.01-2 $\mu m \cdot a^{-1}$ in solution. It is also interesting to note the different apparent time dependence of the corrosion rate in the two environments. In soil, the corrosion rate decreases according to $t^{0.5}$, whereas in bulk solution the rate is almost constant with time.

3.1.2 Electrochemical Considerations

Uniform corrosion can also be represented by the electrochemistry of the constituent oxidation and reduction reactions in the overall corrosion process. This approach has been used in the Canadian program to describe the uniform corrosion of copper UFC (King and Kolar 2000), and a similar procedure could be adopted for C-steel.

The anodic dissolution of Fe

$$Fe \rightarrow Fe^{2+} + 2e^- \quad (1)$$

is supported by either the cathodic reduction of O_2 or H_2O

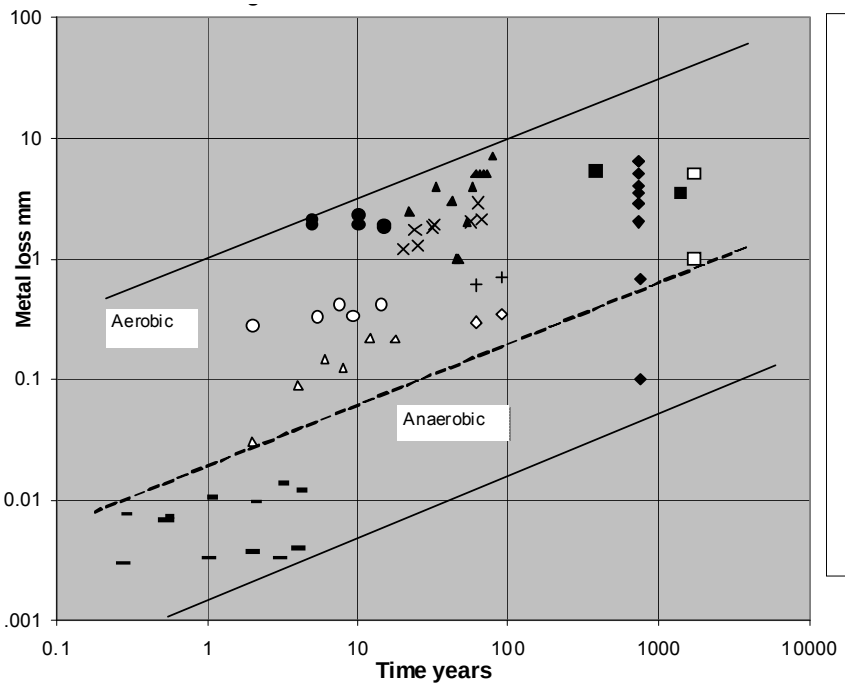
$$O_2 + 2H_2O + 4e^- \rightarrow 4OH^- \quad (2)$$

$$H_2O + e^- \rightarrow \tfrac{1}{2}H_2 \quad (3)$$

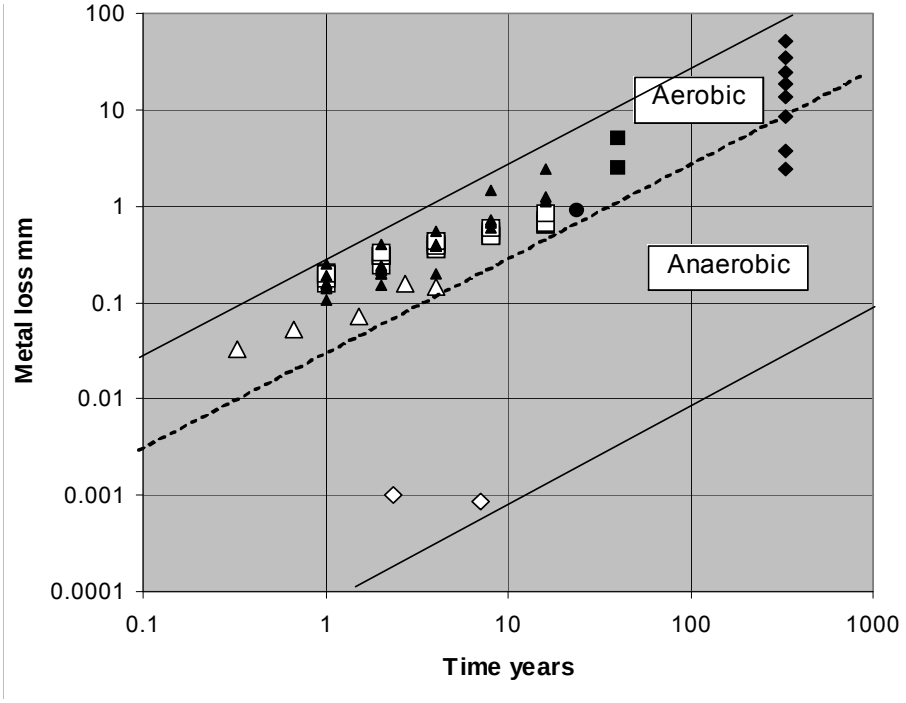
Under aerobic conditions, dissolved Fe^{2+} is rapidly oxidized to Fe^{3+} (Stumm 1992)

$$4Fe^{2+} + O_2 + 2H_2O \rightarrow 4Fe^{3+} + 4OH^- \quad (4)$$

The rates of these individual electrochemical processes have been studied in detail. For instance, there are numerous reports on the dissolution of Fe in Cl^- solutions, including studies by Ashley and Burstein (1991), Chin and Nobe (1977), MacFarlane and Smedley (1986), Marsh and Taylor (1988), Turnbull and May (1987), and You et al. (1993). The kinetics of O_2 reduction on steel has been studied by Calvo and Schiffrin (1988), Gervasio et al. (1998), Gojkovic et al. (1994), Jovancicevic and Bockris (1986), Miyata and Asakura (2002), Stratmann and Müller (1994), Vago and Calvo (1992), Wroblawa and Qaderi (1990), and Zečević et al. (1991a,b).



(a) Soil



(b) Bulk solution

Figure 10: Corrosion Rates of Carbon Steel and Cast Iron from Archaeological Analogs (Crossland 2005).

The mechanism of H_2 evolution has been the subject of extensive study, and useful reviews are given by Bockris and Reddy (1970) and Kaesche (1985). The overall reaction is a two-stage process, involving first the formation of adsorbed hydrogen atoms (H_{ADS})

$$H_2O + M + e^- \rightarrow MH_{ADS} + OH^- \quad (5)$$

where M is a surface metal site. The second stage may follow one of two routes depending on a number of factors, including the nature of the surface, potential, and the surface coverage by H_{ADS}. The so-called Volmer-Tafel route involves the surface recombination of two MH_{ADS} species

$$2MH_{ADS} \rightarrow H_2 + 2M \quad (6)$$

whereas the Volmer-Heyrovsky mechanism involves reaction between MH_{ADS} and H_2O

$$MH_{ADS} + H_2O + e^- \rightarrow H_2 + M + OH^- \quad (7)$$

Kinetic parameters describing the rates of these anodic and cathodic electrochemical reactions are available in the references cited. Sufficient information is available, therefore, to develop a mixed-potential model (MPM) for the prediction of the corrosion potential (E_{CORR}) under film-free conditions. An initial attempt to develop such a model is described by King and Kolar (1999, 2001).

The overall reactions for the corrosion of C-steel are

$$4Fe + 2H_2O + 3O_2 \rightarrow 4\text{"FeOOH"} \quad (8)$$

and

$$Fe + 2H_2O \rightarrow Fe(OH)_2 + H_2 \quad (9)$$

under aerobic and anaerobic conditions, respectively. The species "FeOOH" is used to describe a generic hydrated ferric oxyhydroxide species with an arbitrary number of waters of hydration. Because of the presence of groundwater anions (e.g., Cl^-, SO_4^{2-}, CO_3^{2-}), various types of green rust are more likely to form under aerobic conditions (King and Stroes-Gascoyne 2000).

As the environment becomes anoxic, the Fe(III) corrosion products will be converted to Fe(II) via:

$$2FeOOH + Fe + 2H_2O \rightarrow 3Fe(OH)_2 \quad (10)$$

Under anaerobic conditions, $Fe(OH)_2$ may not be the stable corrosion product, especially at higher temperatures (>80°C). Ferrous hydroxide can decompose to magnetite via the Schikkor reaction

$$3Fe(OH)_2 \rightarrow Fe_3O_4 + 2H_2O + H_2 \quad (11)$$

In addition to modifying the corrosion rate, the formation and alteration of these films will affect the value of E_{CORR}. Precipitated surface films will have a number of effects on E_{CORR}, including:

1. blocking surface sites and reducing the effective surface area for anodic and/or cathodic reactions
2. restricting the mass transport of species to and from the reactive surface
3. potentially catalyzing the rates of O_2 reduction and/or H_2 evolution
4. spatially separating anodic and cathodic reactions
5. galvanically coupling to the underlying C-steel
6. participating in redox reactions, resulting in both changes to the oxidation state of film species and also of species in the bulk environment

Blocking the surface has no effect on the value of E_{CORR} if both anodic and cathodic reactions are equally affected, although the corrosion rate will be lower. If, however, the relative surface areas for the two electrochemical reactions changes then E_{CORR} will either shift to more-positive (higher cathodic surface area) or more-negative (higher anodic surface area) values. These effects were included in the modified C-steel MPM described by King and Kolar (2001), as were the effects of restricting the mass transport of species to and from the underlying C-steel surface. Catalysis of either the O_2 reduction or H_2 evolution reactions will cause a positive shift in E_{CORR} and an increase in corrosion rate, whilst spatially separating anodic and cathodic sites or galvanically coupling film processes to dissolution of the underlying C-steel will induce localized corrosion. Finally, participation in redox processes will also affect the value of E_{CORR}, shifting in either direction, depending upon the nature of the processes involved.

No detailed studies have been performed of the evolution of E_{CORR} for C-steel in a DGR. Compounding the complexity of the various processes described above is the fact that the environment evolves over time. An example of the evolution of E_{CORR} of film-covered C-steel is shown in Figure 11 (Qin et al. 2004). In this example, the film is a layer of millscale produced during the steel-making process, comprising a mixture of Fe_3O_4, $FeCO_3$, and maghemite (γ-Fe_2O_3). This mixture of Fe(II) and Fe(III) species imparts a degree of electrical conductivity to the film and it participates in various electrochemical reactions. The film is also cracked and defected. For the experiment shown, the film-covered C-steel electrode was immersed in a dilute groundwater solution purged with CO_2.

Various electrochemical processes occur during the course of the experiment. Exposure of the sample to this environment causes the millscale layer to slowly dissolve. Initially, the potential appears to be determined by redox processes between the Fe_3O_4 and γ-Fe_2O_3 phases and dissolved Fe(II) in solution (Stage I). After a period of exposure, E_{CORR} decreases precipitously before reaching a second steady-state value in Stage III. During Stage II, it is believed that the reductive dissolution of Fe(III) in the millscale is galvanically coupled to dissolution of Fe in the underlying steel, which becomes possible as the pores and cracks in the film are opened by dissolution of the oxide. As the pores become increasingly larger, the dominant electrochemical reactions become the dissolution of Fe as Fe(II) coupled to the reduction of H_2O, with both occurring over the same surface area, presumably at the base of the pores now opened by further oxide dissolution (Stage III). Note that the value of E_{CORR} in Stage III is identical to that of a film-free C-steel electrode, also shown in Figure 11.

The data in Figure 11 are shown for illustrative purposes, but are thought to be representative of the evolution of E_{CORR} of a C-steel UFC in the repository. As for the Cu UFC, the development of a mixed-potential model for C-steel would not only provide justification for long-term predictions of the rate of uniform corrosion, but would also permit the prediction of the duration during which localized corrosion or SCC is possible.

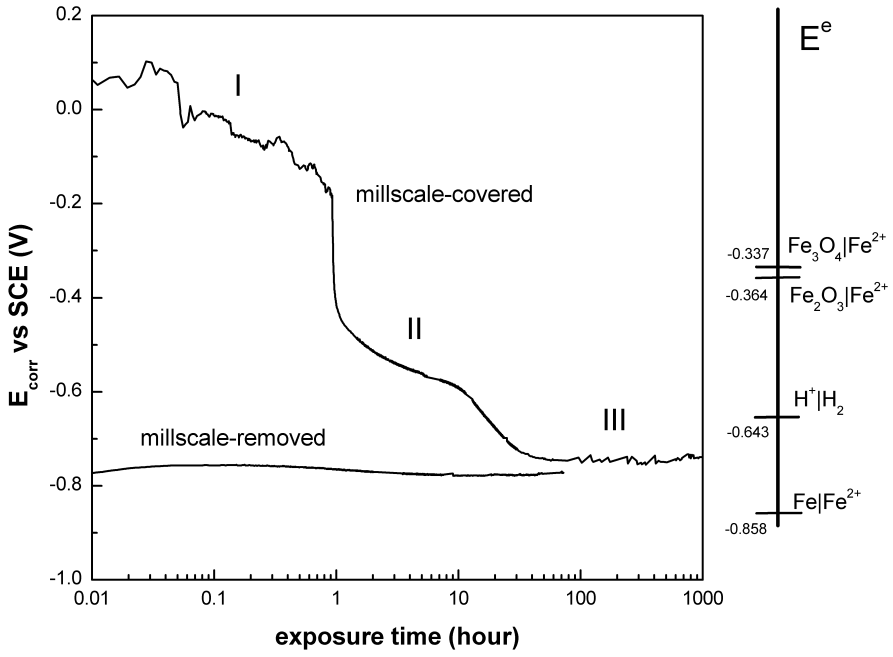


Figure 11: Time Dependence of the Corrosion Potential of a Millscale-Covered C-steel Electrode in CO_2-Containing Solution (Qin et al. 2004).

3.1.3 Gas Generation and Transport

Under anaerobic conditions, uniform corrosion of C-steel is accompanied by the generation of H_2. The overall reaction for the corrosion of C-steel is given by Equation (9), from which it can be seen that 1 mole of H_2 is produced for each mole of Fe corroded. However, if the corrosion product from Reaction (9) (i.e., $Fe(OH)_2$) reacts further to produce Fe_3O_4 via the Schikkor reaction (Equation (11)), an additional 0.33 mole of H_2 is produced for each mole of Fe corroded. It is important, therefore, to understand the nature of the long-term stable corrosion product for C-steel.

The H_2 generated by corrosion will be transported away from the container surface via a number of mechanisms. Some will be absorbed by the C-steel and diffuse through the container wall. The remainder will accumulate at the UFC/buffer interface and be transported away from the container. Because of the limited solubility of H_2 in water and because of the restrictive mass-transport of dissolved species through compacted bentonite, the rate of diffusive transport of H_2 away from the container surface is limited. Based on estimates reported by Nagra (2002), the maximum diffusive flux of H_2 away from the container surface is equivalent to a corrosion rate of <<0.1 $\mu m \cdot a^{-1}$. At higher corrosion rates a secondary H_2 gas phase will form. Transport of gaseous H_2 through compacted bentonite occurs above a threshold gas pressure approximately equal to the sum of the swelling and hydrostatic pressures (Nagra 2002). The exact mechanism of transport is uncertain, but may involve micro-fracturing and pathway dilation, although capillary flow is although believed possible (Nagra

2002). However, regardless of the exact transport mechanism, the overall sealing properties of the bentonite are not believed to be compromised by gas transport, and the permeability returns to its original value once the H_2 pressure is released.

Hydrogen gas transported through the bentonite must also be transported through the low-permeability host rock (King 2005b). Based on the analysis performed by Nagra (2002), the following conclusions can be drawn for the transport of gas in the Ordovician shale and limestone sedimentary deposits (Figure 12):

- As for Opalinus Clay, transport of dissolved H_2 through the shale or limestone is unlikely to transport H_2 away from the repository fast enough to avoid the formation of gaseous H_2 because of the low hydraulic conductivity of the rock formations. However, advection may be possible along the more-conducting Manitoulin Dolostone formation (hydraulic conductivity of 10^{-8} $m \cdot s^{-1}$) that overlays the Queenston Shale.
- Two-phase flow is possible in the sedimentary deposits if the pressure exceeds the break-through pressure (the sum of the hydrostatic and gas-entry pressures). For Opalinus Clay, the gas-entry pressure is of the order 5-10 MPa (Nagra 2002), so assuming the same range for the sedimentary deposits, two-phase flow may occur once the H_2 pressure exceeds 11-16 MPa, for a repository at a depth of 600 m, for example. Two-phase flow will cause gas to flow along some of the existing pore pathways, but does not in itself alter the structure of the sedimentary deposit.
- Pathway dilation, on the other hand, does involve the slow creation of additional microscopic gas pathways, and can occur if the pressure rises because two-phase flow cannot remove the H_2 fast enough.
- Gas fractures can form when the H_2 pressure builds up quickly and involves the formation of microscopic channels and occurs when the gas pressure exceeds the tensile strength of the host rock. Based on the data provided by Golder (2003), this would occur at a pressure of ~20 MPa (tensile strength plus lithostatic load). This mechanism requires the rapid generation of H_2 pressure, which will not occur in a deep geological repository for any realistic corrosion rate.

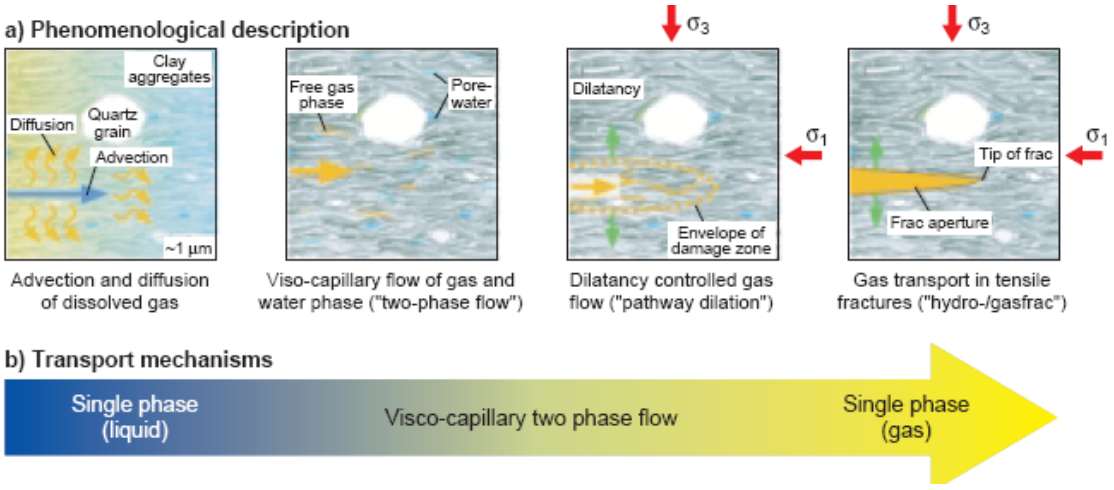


Figure 12: Schematic of Gas Transport Mechanisms in Opalinus Clay (Marschall et al. 2005).

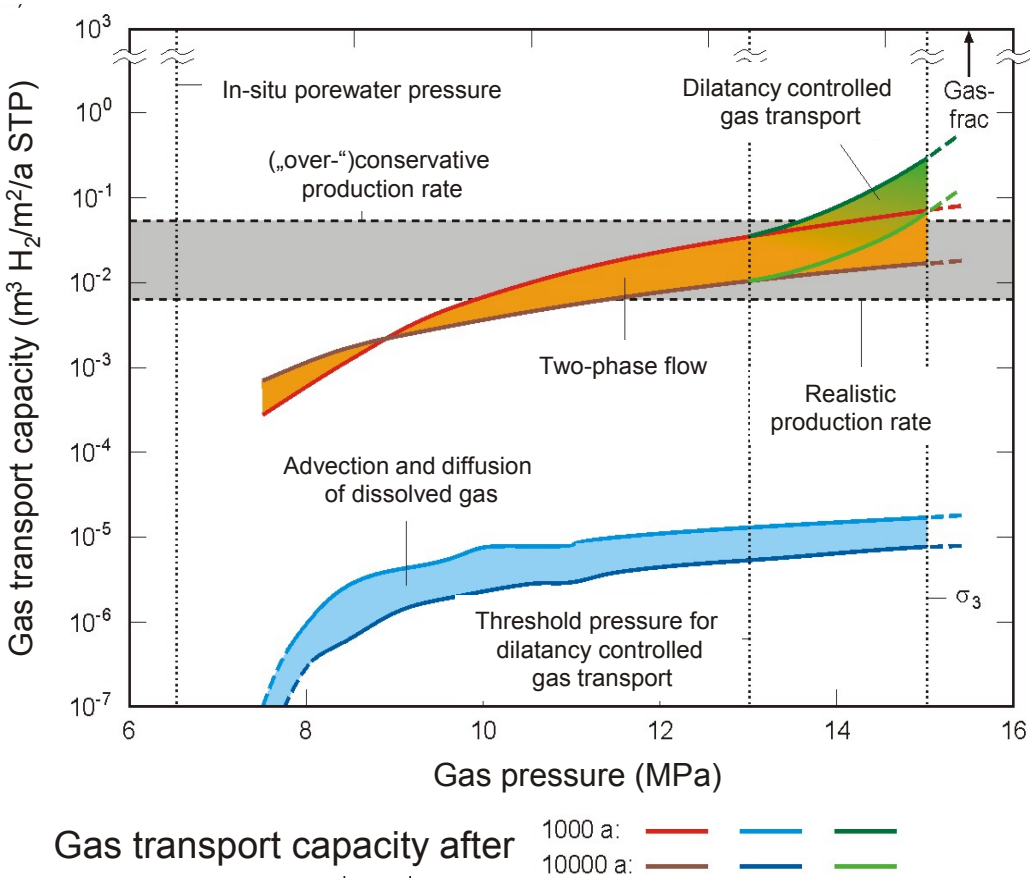


Figure 13: Gas Transport Capacity for Various Gas Transport Mechanisms in Opalinus Clay as a Function of the Total Pressure (Nagra 2004).

Figure 13 shows the gas transport capacity in Opalinus Clay for various mechanisms as a function of the gas pressure. The gas transport capacity represents the rate at which gas (e.g., H_2) can be transported through Opalinus Clay, and can alternatively be expressed in terms of a corrosion rate. The horizontal shaded area in Figure 13 represents a range of corrosion rates of 1-10 $\mu m \cdot a^{-1}$, approximately the range expected for the long-term anaerobic phase. It is clear, therefore, that advection and diffusion of dissolved gas (the blue shaded area) will not remove gas fast enough from the UFC surface to prevent the formation of a secondary gas phase. Two-phase flow, possibly with some degree of dilatancy-controlled transport will be able to remove H_2 at the expected generation rate, however. Transport by gas fracs, on the other hand, would require a corrosion rate 3-4 orders of magnitude higher still (L.H. Johnson, private communication 2007).

It appears, therefore, that H_2 gas generated by corrosion will exist in both the dissolved and gaseous forms at the UFC surface during the anaerobic phase in the evolution of the repository environment. However, this gas can be removed by a combination of diffusion and two-phase flow (and, possibly, some pathway dilation), but will not compromise the sealing and mass-transport properties of the compacted bentonite or sedimentary host rock.

3.2 LOCALIZED CORROSION

By definition, localized corrosion results from the spatial separation of anodic and cathodic reactions, resulting in the localized dissolution of the metal. Classically, localized corrosion occurs as a result of the breakdown of a passive film, whereby the majority of the surface is protected from corrosion and dissolution occurs preferentially at defects in the passive layer (Szklarska-Smialowska 2005). It is uncertain whether the surface of a C-steel UFC will be passive or not. Japanese studies in compacted bentonite (JNC 2000) suggest that the surface is active, an observation that is consistent with the expected pore-water pH value of pH 7-8 (King 2005b). As illustrated in Figure 14, C-steel (or Fe) will passivate due to the formation of a Fe_3O_4 film in the pH range pH 7-9, depending upon potential (based on the equilibrium between Fe_3O_4 and a 10^{-6} mol·dm^{-3} Fe(II) solution). Under relatively oxidizing conditions (e.g., -0.25 V_{SHE} or –0.5 V_{SCE}), Fe_3O_4 will is thermodynamically stable at ~pH 7. Conversely, under anaerobic conditions (e.g., -0.55 V_{SHE} or –0.8 V_{SCE}), the equivalent pH is ~pH 8.5.

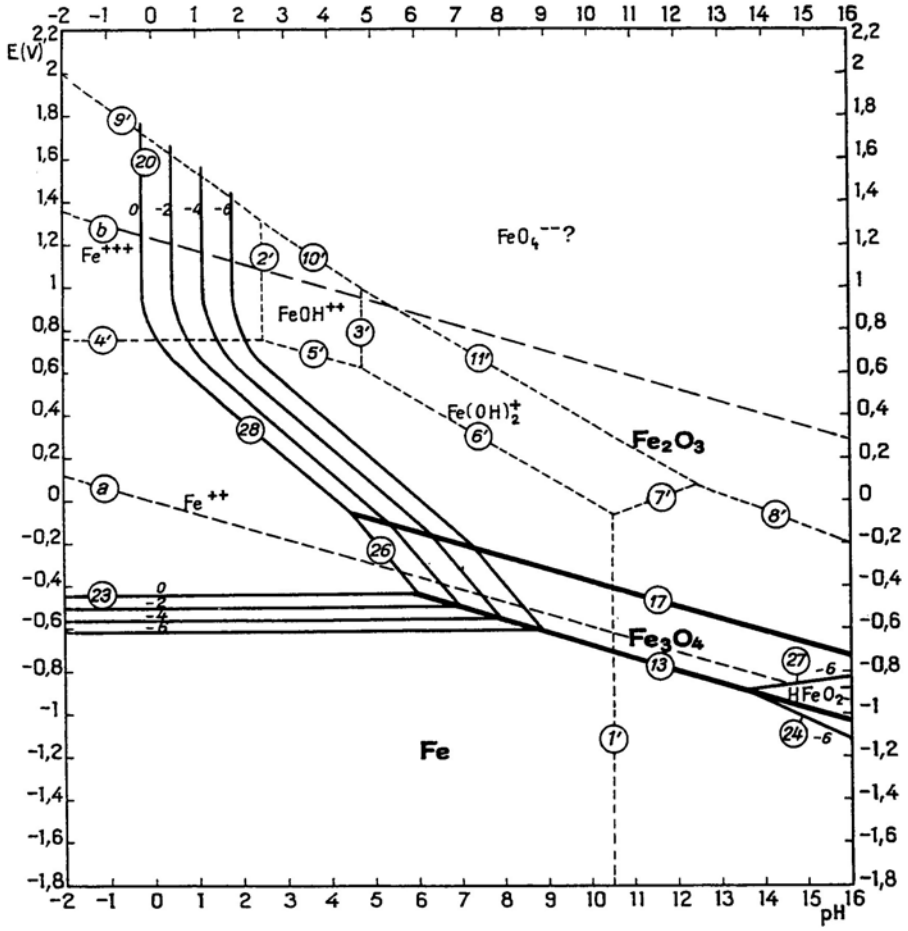


Figure 14: Potential-pH Diagram for the Fe-H_2O System at 25°C (Pourbaix 1974).

Localized attack, however, can be induced by other processes, such as the inhomogeneous distribution of environmental conditions. For example, a non-uniform flux of O_2 to the container surface, or the presence of chemical gradients due to the inhomogeneous distribution of mineral impurities in the clay or local mass-transport gradients. Under such circumstances, however, if the surface is not inherently passive then attack tends to be in the form of uneven uniform corrosion.

3.2.1 Mechanisms of Localized (Pitting) Corrosion of C-steel UFC

A number of different mechanisms can be postulated under which a certain degree of localized attack of the surface could occur. The possible localized (pitting) corrosion mechanisms discussed here are: (i) non-uniform wetting of the surface during the initial cooling phase following the peak in UFC surface temperature, (ii) localized breakdown of a passive film, and (iii) reductive dissolution of an Fe(III)-rich film during the transition from aerobic to anaerobic conditions.

During the initial thermal transient, the UFC surface will first dry out and then re-wet as the temperature drops and the %RH in the bentonite pores increases. Wetting of the UFC will first occur as a result of the deliquescence of (salt) impurities on the surface of the container (King 2006). Deliquescence of isolated salt crystals will cause the spatial separation of anodic and cathodic sites, with the anodic reaction located under the water droplet condensed on the salt particle and the cathodic reaction restricted to the periphery of the droplet and in satellite micro-droplets (Figure 15). The degree of localized corrosion will depend on a number of environmental factors, including:

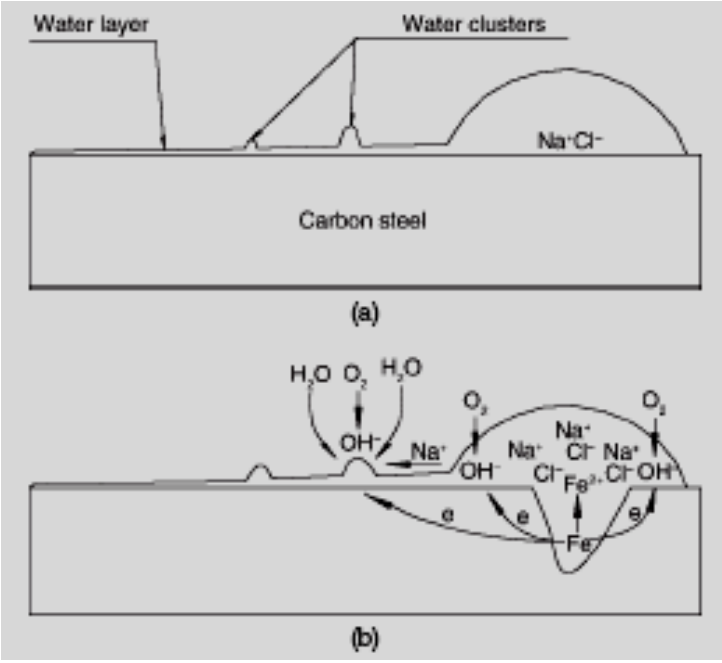
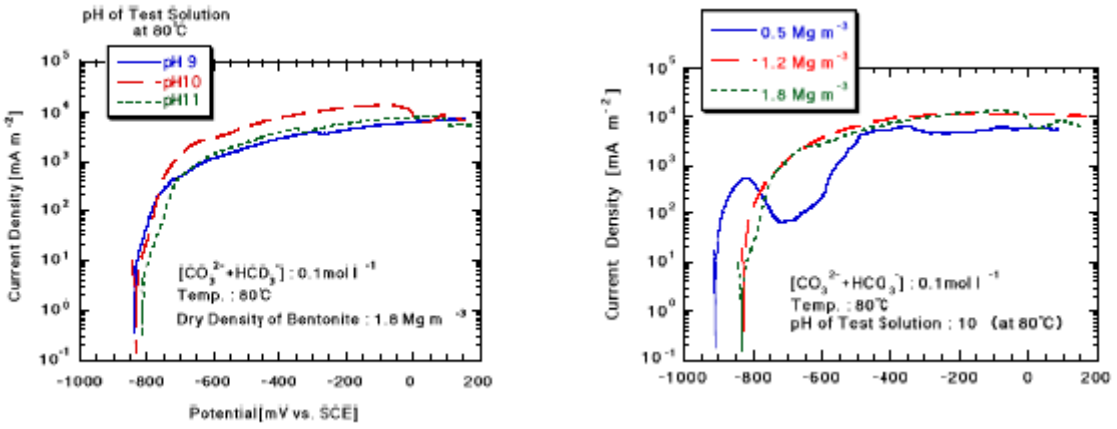


Figure 15: Proposed Mechanism for the Distribution of Anodic and Cathodic Reactions for Micro- and Large Droplets of Water (after Zhang et al. 2005).

1. the surficial density of contaminants, with less localized attack the greater the density of salt crystals,
2. the rate of increase in the %RH, and
3. the duration of the aerobic phase.

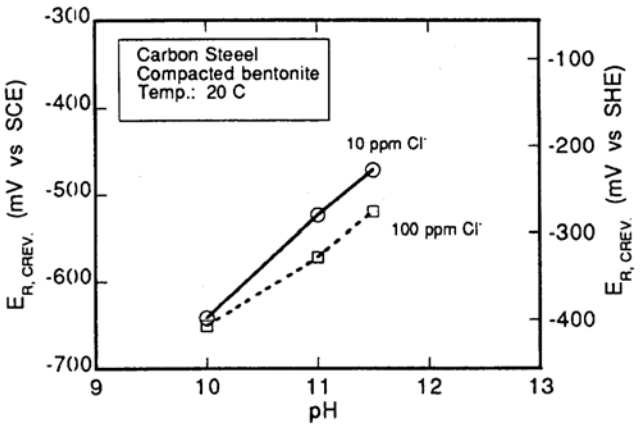
The driving force for localized corrosion via this non-uniform surface wetting mechanism will diminish with time as the surface becomes more-evenly wetted. Separation of anodic and cathodic sites results from the greater access of O_2 to the C-steel surface around the periphery of the droplets and to the micro-droplets and thin surface film connecting the micro-droplets to the main droplet (King 2006). As the %RH increases, the surface will become increasingly wetted and the solution in the droplet will become more dilute. More uniform wetting results in uniform access of O_2 and the loss of the spatial separation of anodic and cathodic reactions. As the environment evolves, therefore, the natural tendency will be for this form of localized corrosion to stifle.

Classical localized corrosion due to the breakdown of a passive film requires that the UFC surface be passive. Japanese workers have studied the passivity of C-steel in compacted 70:30 bentonite:sand buffer as a function of pore-water pH and buffer density (Figure 16). In dense buffer material (dry density 1.8 $Mg \cdot m^{-3}$), voltammetric scans suggest active behaviour in the range pH 9-11 (Figure 16(a)). At a constant pH 10, passivity is observed at dry densities of 1.2 $Mg \cdot m^{-3}$ and 1.8 $Mg \cdot m^{-3}$, but not at 0.5 $Mg \cdot m^{-3}$. No explanation was given for this latter effect, but it may reflect the lower pH-buffering capacity of the relatively unconsolidated buffer. Ion-exchange and equilibration with calcite impurities in the bentonite are likely to result in a decrease in the initial pore-water pH to values closer to the pH 7-8 range.

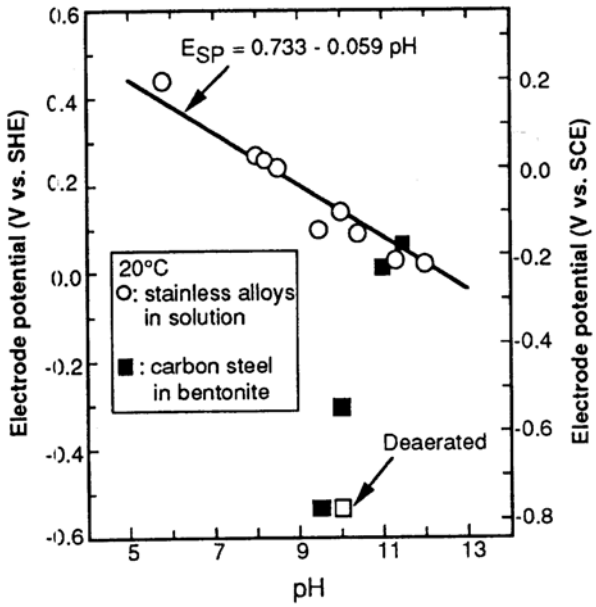


(a) Effect of pore-water pH **(b) Effect of buffer density**

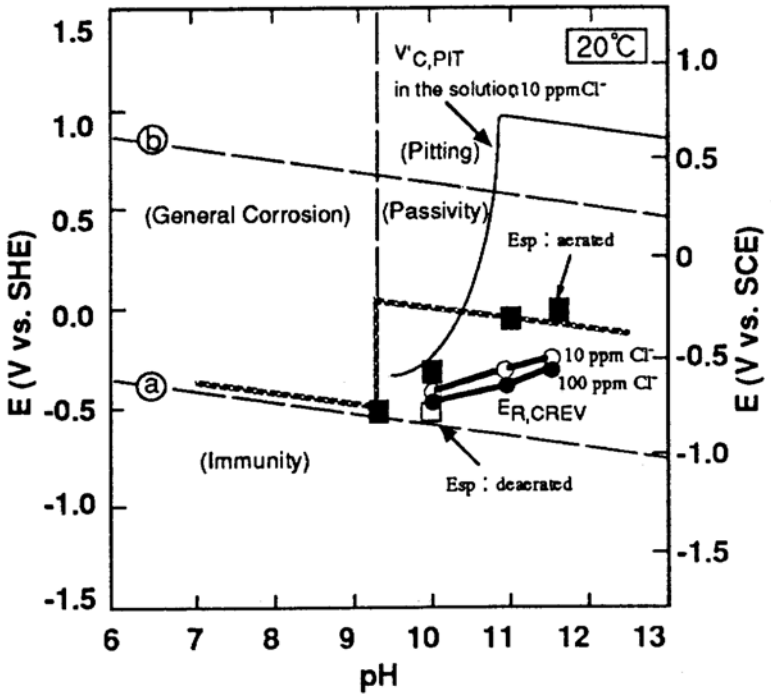
Figure 16: Anodic Polarization Curves for C-steel in Compacted 70:30 Bentonite:Sand Buffer Material (JNC 2000).



(a) Crevice re-passivation potential



(b) Corrosion potential



(c) Comparison of re-passivation and corrosion potentials

Figure 17: Dependence of Repassivation Potentials for the Pitting and Crevice Corrosion of Carbon Steel on pH (Fukuda et al. 1995).

Fukuda and Akashi (1995) and Fukuda et al. (1995) report a critical pH (in bulk solution) of ~pH 9.5 at 20°C above which C-steel is passive (Figure 17). This pH value is lower than the initial pore-water pH values in the compacted buffer tests in which only active behaviour was reported (Figure 16), further suggesting that the pore-water pH in these latter tests is modified by interaction with the clay minerals. Fukuda et al. (1995) also determined the values of the re-passivation potential for creviced C-steel samples ($E_{R,CREV}$, Figure 17(a)) and the value of E_{CORR} in aerated and deaerated solution (Figure 17(b)), both as a function of pH.

Comparison of these data suggest that localized corrosion due to the breakdown of a passive film is unlikely to occur for a C-steel UFC in compacted buffer material. The value of E_{CORR} only exceeds $E_{R,CREV}$ at pH > 9.5 and then only in aerated solution. As with the deliquescence-induced localized corrosion mechanism described above, this mechanism also becomes less likely as the environment evolves and conditions becomes anaerobic.

The third possible mechanism for localized corrosion considered here occurs during the transition from aerobic to anaerobic conditions. Reductive dissolution of Fe(III) corrosion products could become coupled to the dissolution of the underlying C-steel exposed at pores or cracks in the corrosion product layer (Figure 18(a)). This coupled process would occur during Stage II in the evolution of E_{CORR} illustrated in Figure 11 or, in other words, during the transition from aerobic to anaerobic conditions in the repository. Evidence for such coupled processes is widespread in the literature (e.g., Shoesmith et al. 1981).

The duration of this localized corrosion mechanism depends on: (i) the quantity, exposed surface area, and rate of reduction of Fe(III) corrosion product, (ii) the relative rates of Fe(III) reduction and the reduction of H_2O, and (iii) the rate of pore-opening and increasing surface area of exposed C-steel. Rapid rates of localized penetration will only occur if the small anode:large cathode geometry is maintained. As the pores in the Fe(III) corrosion product layer increase in size due to dissolution of the layer, the overall cathodic current will become increasingly dominated by the reduction of H_2O on the exposed C-steel layer at the base of the pores (Figure 18(b)). Under these circumstances, the anodic and cathodic reactions are occurring in the same location and corrosion becomes uniform in nature. Again, therefore, this localized corrosion mechanism is transitory and tends to stifle with time.

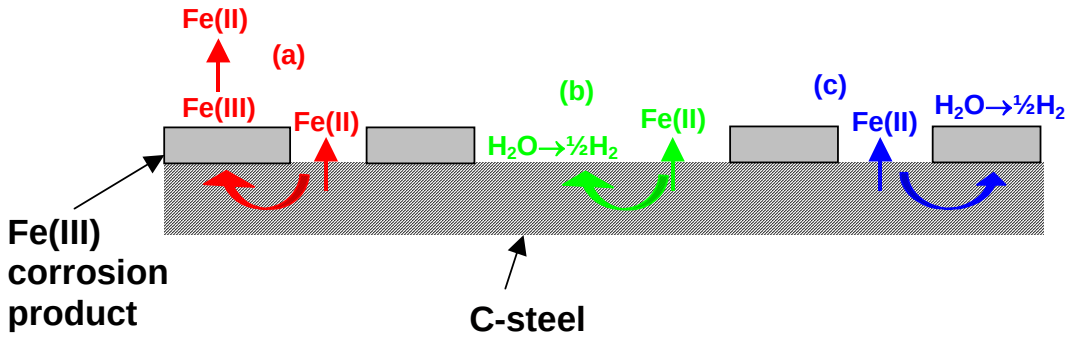


Figure 18: Illustration of Possible Spatial Locations for Anodic and Cathodic Reactions on a Film-covered C-steel Surface.

There are other possible localized corrosion mechanisms not considered in detail here. For example, O_2 diffusion to the UFC surface could be inhomogeneous if the buffer is unevenly compacted or placed or if uneven swelling develops. Another example is the catalysis of H_2O reduction on areas of the surface covered by Fe_3O_4 coupled to Fe dissolution in pores or cracks in the film (Figure 18(c)). Jack et al. (2003) report evidence for faster H_2O reduction kinetics on millscale-covered surfaces than on polished C-steel. (Millscale is a mixture of Fe(III) corrosion products and Fe_3O_4 resulting from the manufacture of steel, and may be electrochemically similar to a Fe_3O_4-covered surface).

In summary, it is difficult to exclude the possibility of some form of localized dissolution of a C-steel UFC in the repository environment. However, in all cases, the driving force for localized corrosion diminishes with increasing time. Localized corrosion, therefore, is only of concern during the initial period in the evolution of the repository environment. After the establishment of stable, long-term anaerobic conditions, corrosion will be uniform in nature.

3.2.2 Treatment of Initiation and Propagation

There are a number of methods for predicting the localized corrosion behaviour of C-steel UFC. These methods can be broadly classified as relating to either the initiation of localized corrosion or the propagation of damage following initiation. Predictions based on initiation are useful if it expected that the UFC will be immune to localized corrosion, or only susceptible for a short period of time or under a limited set of conditions. Propagation models are useful when initiation is assumed but the extent of damage is thought to be limited, again either because of limitations of time or environment or because the material properties are such that the propagating pit or crevice will stifle (cease to grow). In the case of C-steel and the various mechanisms proposed above, both initiation and propagation arguments are appropriate.

As briefly described above, initiation of localized corrosion is typically predicted based on a comparison of the corrosion potential E_{CORR} and the re-passivation potential E_{RP}. Localized corrosion is assumed to initiate if the following condition is met:

$$E_{CORR} \geq E_{RP} \tag{12}$$

This approach is conservative, since initiation actually occurs at the breakdown potential E_B, which is typically 50-200 mV more-positive than E_{RP}. The re-passivation potential is actually the potential at which an already initiated pit ceases to grow (i.e., re-passivates) (Szklarska-Smialowska 2005).

This approach requires a knowledge of the (time-dependent) E_{CORR} of the container and of the value(s) of E_{RP} under a range of relevant environmental conditions. This approach has been extensively used in the U.S. Yucca Mountain Project for the prediction of localized corrosion of Alloy 22 (see, for example, Gordon 2002, King and Kolar 2006) and has also been implicitly used for the prediction of the pitting of Cu UFC (King 2002, 2004; King et al. 2001, 2002).

Re-passivation data for C-steel are available in the literature or could be generated from specific experimental studies. Data can be measured on free surfaces, in which case the E_{RP} is referred to as a pitting re-passivation potential $E_{RP,PIT}$, or using samples with artificial crevices, in which case one measures the crevice re-passivation potential $E_{RP,CREV}$. Because it is easier to separate anodic and cathodic reactions (and, hence, initiate localized corrosion) if there is a geometric discontinuity such as a crevice, $E_{RP,CREV}$ is typically more negative than $E_{RP,PIT}$, and

therefore provides a more-conservative assessment of localized corrosion initiation. In both cases, however, the value of the re-passivation potential is dependent on environmental conditions (e.g., temperature, $[Cl^-]$, $[HCO_3^-/CO_3^{2-}]$, etc.) and also exhibits variability due to experimental factors, such as the surface preparation method, method of forming and tightness of crevice, etc. Therefore, E_{RP} values are best described as a probability density function.

Sources of re-passivation potentials in the literature include the compilation of Szklarska-Smialowska (2005), in addition to numerous other individual studies. A key role is played by the pH of the environment, with uniform corrosion observed below a critical pH (pH_{CRIT}) and localized corrosion possible at higher pH (Brossia and Cragnolino 2000). The value of pH_{CRIT} depends on the temperature and the concentration of ions in solution, and has been reported to range from pH 8 to pH 10.5 (Bird et al. 1988, Fukuda and Akashi 1995, Makar and Tromans 1996, Marsh and Taylor 1988). Species such as Cl^- and SO_4^{2-} promote localized film breakdown, whereas HCO_3^-/CO_3^{2-} and increasing pH promote passivity.

The other required parameter is the corrosion potential of the container. Although E_{CORR} can be measured during laboratory experiments (e.g., Figures 11 and 17(b)), the long-term E_{CORR} behaviour is best predicted using a mixed-potential model, as has been carried out for Cu (King and Kolar 2000).

Propagation of localized corrosion can be predicted in a number of ways (Turnbull 1993). These methods can be broadly classified as either empirical or mechanistic in nature. Empirical models make use of measured parameters, such as current transients from electrochemical experiments or direct measurements of damage from simple immersion tests, to extrapolate into the future. For empirical models, the key factor is whether the environments in which the measurements were made are representative of the service conditions for which the prediction is required. Mechanistic models, as their name suggests, are based on the mechanism of the pitting or crevice corrosion process. These models typically account for the electrochemical, chemical, mass transport, and (sometimes) precipitation/dissolution reactions inherent in the overall corrosion process. As such, the effects of many different environmental factors can be taken into account, provided the mechanism is sufficiently well understood.

In reviewing these modelling approaches, Turnbull (1993) concluded that the best approach to predicting localized corrosion propagation was through a combination of empirical and mechanistic modelling. Predictions of corrosion damage are best made using empirical techniques, but the understanding derived from mechanistic models is essential for assessing the robustness of the predictions and for providing insights into the empirical data.

The Japanese (JNC 2000) and Swiss (Johnson and King 2003) nuclear waste management programs have made use of an extensive database of pitting factors derived from a long-term underground corrosion study carried out by the U.S. National Bureau of Standards (Romanoff 1989). Similar databases exist in the pipeline industry (e.g., Katano et al. 2003, Martinsek 2003), although these latter sources have not yet been incorporated into predictions of UFC lifetimes.

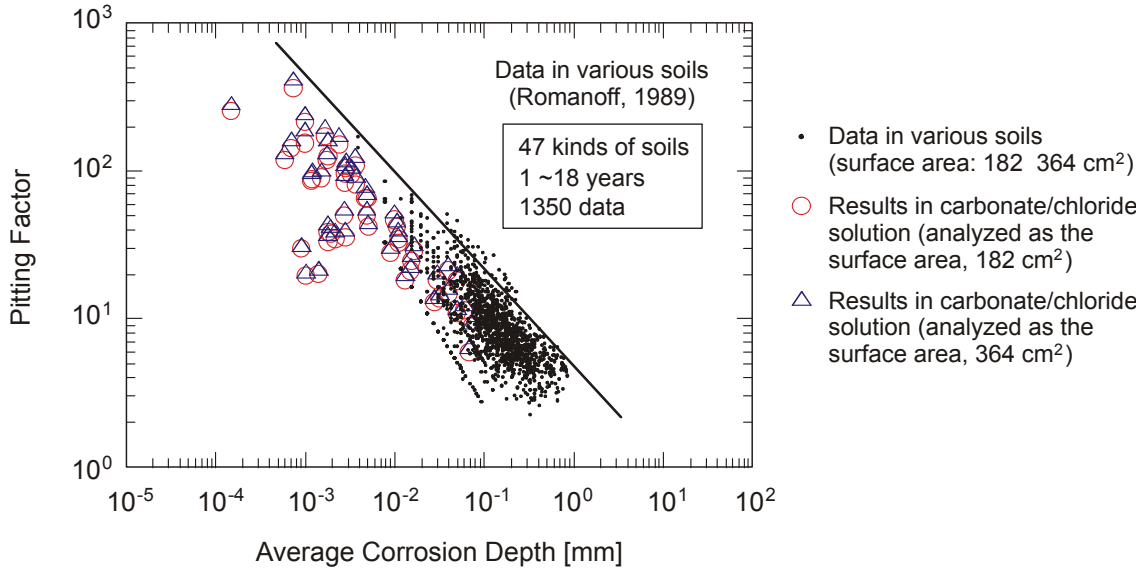


Figure 19: Relationship Between the Pitting Factor and the Mean Corrosion Depth for Carbon Steel Exposed to Various Environmental Conditions (JNC 2000, Johnson and King 2003).

Figure 19 shows the variation in pitting factor (the ratio of the depth of the deepest pit to the mean depth of corrosion) as a function of the mean corrosion depth. This impressive data set of ~1400 points clearly shows that the degree of roughness diminishes with increasing depth of corrosion. In other words, what starts off as localized corrosion transforms into uneven uniform corrosion with time. This tendency for localized corrosion to stifle can also be expressed as

$$D = kt^n \qquad (13)$$

where D is the maximum depth of corrosion, k is a constant, and the time (t) exponent n has a value of <1.

From a mechanistic standpoint, the value of n < 1 could have a number of causes, including:

1. iR drop down the pit or crevice, reducing the potential driving force for dissolution
2. limitation by diffusion into or out of the pit or crevice
3. loss of critical crevice/pit chemistry
4. dissolution of un-passivated crevice/pit walls resulting in a decrease in aspect ratio

This is an example of how a mechanistic understanding of the detailed corrosion processes can support the use of empirical data for lifetime prediction. The data in Figure 19 have been used to predict the depth of localized corrosion for C-steel UFC in both the Japanese (JNC 2000) and Swiss programs (Johnson and King 2003) and, in a preliminary fashion, in the Canadian program (King 2005a).

3.3 HYDROGEN EFFECTS

3.3.1 Hydrogen Degradation Mechanisms in Carbon Steel

A number of hydrogen-related degradation mechanisms have been identified for C-steel (Craig 1987), including: (i) embrittlement during plastic deformation due to exposure to gaseous H_2, (ii) hydrogen stress cracking (also referred to as hydrogen-induced cracking (HIC) and, in sulphide-containing environments, sulphide stress cracking), (iii) the loss of ductility during plastic deformation, (iv) high-temperature hydrogen attack, (v) blister formation, (vi) damage due to hydrogen picked up during casting and forging, (vii) hydrogen cracking of welds, and (viii) degradation of creep properties.

Of these mechanisms, a number can immediately be excluded from consideration as not being relevant under repository conditions (Craig 1987). First, neither H embrittlement in gaseous H_2 nor high-temperature H attack will occur at repository temperatures. Second, processes such as the loss of ductility during plastic deformation and the degradation of creep properties by H can be avoided through proper UFC design that limits plastic strain or creep due to external loading. Third, the unwanted absorption of H during casting/forging and welding can be avoided through proper specification of procedures and weld consumables.

Consequently, the two H degradation mechanisms of most concern are

1. hydrogen stress cracking (of hydrogen-induced cracking), in which H accumulates under a stress gradient leading to internal crack formation, and
2. blister formation, as a result of H accumulation at internal voids, laminations, or inclusions.

These mechanisms have been extensively studied in relation to the use of C-steel in the oil and gas industry. In general, the susceptibility of C-steel to these mechanisms increases with increasing strength of the material and increasing absorbed hydrogen concentration [H] (Figure 20). For these reasons, both JNC (2000) and Johnson and King (2003) argued that both the use of a low-strength steel container and the nature of the repository environment mitigated against hydrogen-related degradation mechanisms. The grade of C-steel for a UFC in the hypothetical DGR in sedimentary rock has not been defined, but as a guide the yield strengths considered by JNC (2000) and Johnson and King (2003) for the Japanese and Swiss UFC were $\leq$635 MPa and 256 MPa, respectively. Based on Figure 20, the maximum "allowable" [H] to avoid hydrogen-related cracking mechanisms would be of the order of 2 $\mu g \cdot g^{-1}$ and 10 $\mu g \cdot g^{-1}$, respectively. In contrast, Figure 21 shows the effect of a number of environmental parameters on the sub-surface [H] determined from hydrogen-permeation tests (King et al. 2005). With the possible exception of HS^-, the concentrations are of the order of 0.2-2 $mol \cdot m^{-3}$ (0.05-0.5 $\mu g \cdot g^{-1}$), approximately one order of magnitude below the "allowable" [H] based on Figure 20. Sulphide results in higher [H] because of the poisoning of the H atom recombination reaction on the surface. The presence of a surface film reduces the concentration of absorbed hydrogen, possibly by blocking surface sites for H formation and subsequent absorption (Jack et al. 2003).

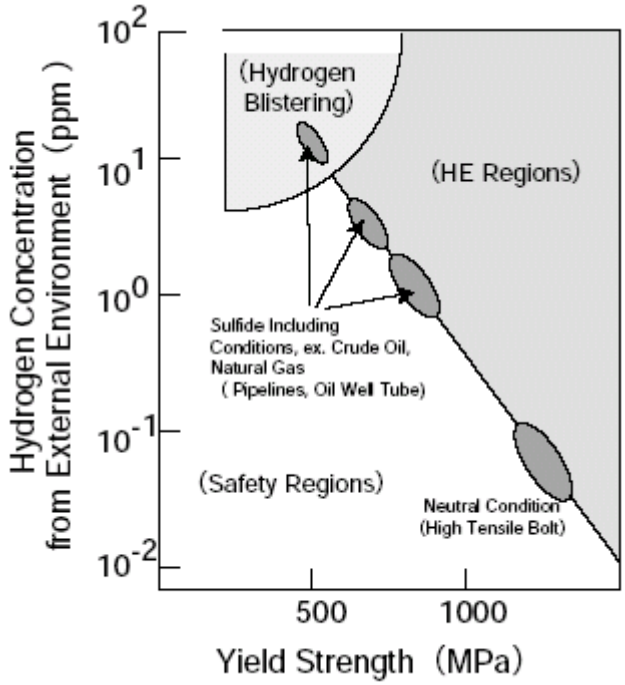
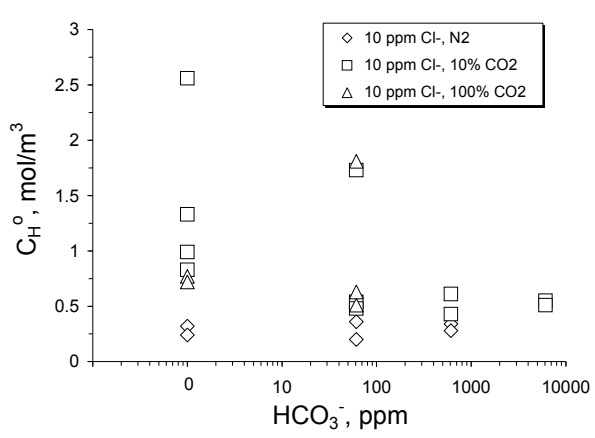
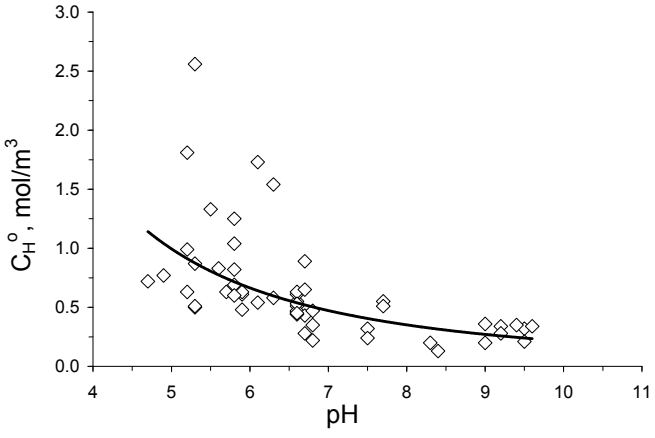


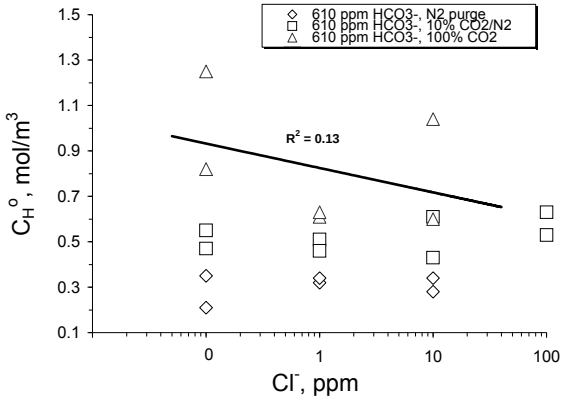
Figure 20: Schematic Illustrating the Zones of Susceptibility of Carbon Steel to Hydrogen-related Degradation Mechanisms Based on the Absorbed Hydrogen Concentration and the Material Yield Strength (JNC 2000).



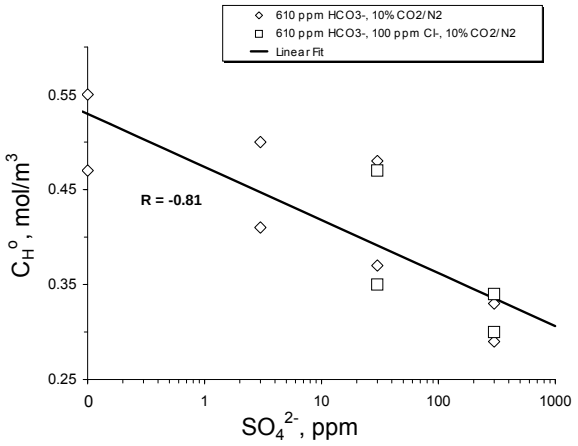
(a) Effect of HCO_3^-



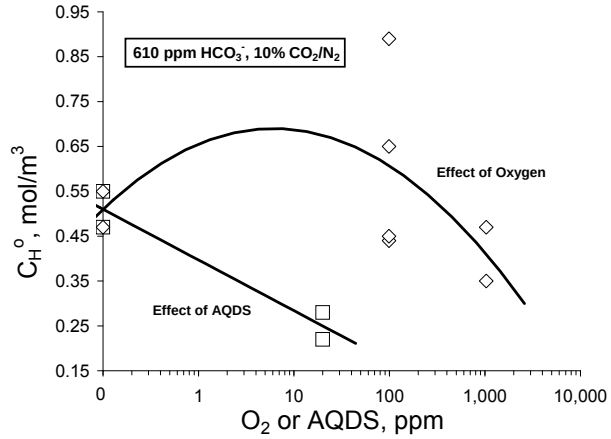
(b) Effect of pH



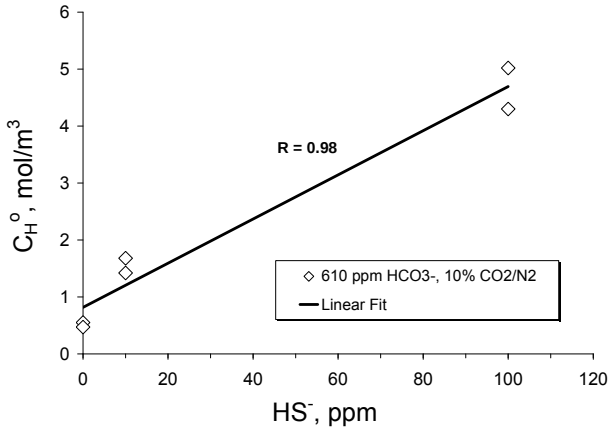
(c) Effect of Cl^-



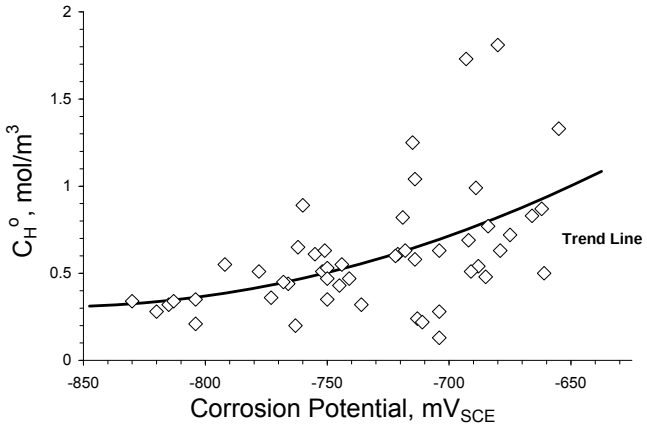
(d) Effect of SO_4^{2-}



(e) Effect of O_2 and AQDS*



(f) Effect of HS^-



(g) Effect of E_{CORR}

Figure 21: Effect of Various Environmental Parameters on the Sub-surface Absorbed Hydrogen Concentration (King et al. 2005).

* AQDS, 9, 10-anthraquinone-2, 6-disulfonic acid, is a model compound for humic acid.

3.3.2 Treatment of Hydrogen Degradation Mechanisms

As noted above, H degradation due to hydrogen stress cracking or blistering can be avoided if the sub-surface absorbed H concentration (c_H^0) is lower than the (temperature-dependent) threshold concentration $(c_H^0)_{TH}$, i.e.,

$$c_H^0 < (c_H^0)_{TH} \quad (14)$$

The data shown in Figures 20 and 21 are for older ferrite/pearlite steels with high concentrations of MnS inclusions. Modern steels, typical of that from which the UFC would be constructed, are designed to be more resistant to hydrogen-induced damage (Hay 2003).

Resistance to H-related effects can be achieved by either lowering c_H^0 or by raising $(c_H^0)_{TH}$. Various alloying elements in low concentrations are found to lower c_H^0 in sour (i.e., H_2S-rich) environments, including:

- Cu at a maximum concentration of 0.35 wt.%, is believed to stabilize protective iron sulphide films,
- Co in the range 0.6-1.0 wt.%, possibly through an effect on the iron sulphide film,
- Ni is believed to lower the corrosion rate and may also inhibit H atom absorption, and
- Cr at a concentration of 0.6 wt.% is found to reduce H atom absorption.

Thus, alloying elements affect the value of c_H^0 by either (i) stabilizing protective iron sulphide films, (ii) lowering the corrosion rate and, hence, the rate of H atom formation, or (iii) reducing the fraction of H atoms absorbed by the steel.

The alternative strategy is to increase the value of $(c_H^0)_{TH}$ (Hay 2003). This strategy involves:

- eliminating MnS inclusions of a certain (Type II) shape, Al_2O_3 particles, anomalous (heavily banded) microstructures, and other non-metallic inclusions (e.g., silicates, slag, Fe oxides, large Nb carbonitride particles),
- reducing the segregation of trace/impurity elements in the steel, and
- increasing the homogeneity of the microstructure.

Type II MnS inclusions are dendritic or rod-like in shape and are associated with deleterious effects on the susceptibility to H damage due to the trapping of H atoms as H_2 molecules. Elimination of Type II MnS inclusions can be achieved by:

- reducing the S content as much as possible (<0.003 wt.% and sometimes <0.001 wt.%)
- a maximum Mn content of 1.00 wt.%, and preferably 0.80 wt.% max., and
- controlling the shape of remaining MnS inclusions.

Shape control is achieved by adding elements that have a higher affinity for S than Mn, such as Ca. In addition, CaS is spherical in shape (Type I) and non-deformable during processing. The optimum Ca:S ratio depends on the S content and whether the material is to be used as plate or as welded or seamless linepipe. For a S content of 0.003 wt.%, the Ca:S ratio should be in the range 1-3.5, with the upper end of the range decreasing with increasing S content.

Alumina particle stringers, or the voids associated with them, are also effective trap sites for H atoms (Hay 2003). The total Al content (including dissolved Al, aluminates, aluminum nitrides, and alumina particles) should not exceed 0.030 wt.%. The formation of alumina can be avoided by

- adding the minimum Al necessary when killing the steel,
- preventing oxidation of Al during casting, and
- preventing the incorporation of alumina particles as the steel solidifies.

Excessive banding in the microstructure (due to the formation of alternating ferrite and ferrite/pearlite bands) can be avoided by controlling the concentrations of C, Mn, and P. Microstructure control can be achieved if the C content is <0.10 wt.%, the P content is <0.015 wt.% (preferably <0.010 wt.%), and the maximum Mn content is 1.00 wt.%.

The content of non-metallic inclusions can be reduced by skimming off prior to solidification.

Reducing the C and Mn content to avoid excessive banding has the adverse effect of reducing the strength of the steel. Micro-alloying elements (such as Ti, Nb, and V) are therefore commonly added to increase the strength through the formation of Ti, Nb, or V carbides. These elements are added to a maximum combined concentration of 0.12 wt.% to avoid the formation of small regions of high hardness in the heat-affected zone (HAZ) of welds.

An alternative strategy for increasing the yield strength, obtaining resistance to H effects, and improving the toughness and weldability of linepipe steel is Thermo-Mechanical Control Processing (TMCP). The overall aim is to produce a steel with a uniform, very clean, fine-grained, non-banded microstructure. In addition to chemical control, this process involves the careful control of temperature during the rolling process. Such steels tend to have a uniform ferrite-bainite microstructure, with no pearlite banding.

The recommended specification for HIC-resistant pressure vessel plate, similar to that from which a C-steel UFC would be manufactured, is (Hay 2003):

Processing:

- minimize use of scrap additions
- desulphurized, dephosphorized, and fully deoxidized (Al-Si killed)
- removal of oxide inclusions (35 ppm O max.)
- addition of Ca for sulphide shape control
- continuous casting
- normalized heat treatment

Chemical composition:

- C 0.18 wt.% max. (UTS $\leq$ 414 MPa), 0.21 wt.% max. (UTS > 414 MPa)
- Mn 1.30 wt.% max.
- Si 0.45 wt.% max.
- P 0.010 wt.% max.
- S 0.002 wt.% max.
- Cu 0.35 wt.% max.
- Ni 0.25 wt.% max.

- Cr 0.25 wt.% max.
- Mo 0.10 wt.% max.
- Total Al 0.040 wt.% max. (preferably <0.030 wt.% max.)
- Nb 0.015 wt.% max.
- V 0.015 wt.% max.
- Ti 0.020 wt.% max.
- B 0.0005 wt.% max.
- Ca 1.8-3.5 x %S
- Nb + V 0.020 wt.% max.

The carbon equivalent (defined as CE = C + Mn/6 + (Cu + Ni)/15 + (Cr + Mo + V)/5) should be limited to the range 0.40-0.47.

Microstructure:

The microstructure should be free of excessive ferrite/pearlite banding.

By controlling the steel chemistry and processing in this manner, it is possible to produce a highly HIC-resistant steel.

3.4 STRESS CORROSION CRACKING

Stress corrosion cracking is a failure mechanism that occurs because of the simultaneous presence of tensile stresses (due to static or cyclic loading conditions), an environment, and a susceptible material. Carbon steel is considered to be susceptible to SCC.

Environments

Carbon steel is susceptible to stress corrosion cracking (SCC) in a number of environments, notably: caustic, nitrate, phosphate, CO-CO_2, high-temperature water (>200^{o}C), and HCO_3^-/CO_3^{2-} (Ciaraldi 1992). Of these causes, a number can be excluded from consideration because the environment will not form in the repository (Johnson and King 2003, King 2005a), particularly nitrate, phosphate, CO-CO_2, and high-temperature water. Because of the pH-buffering capacity of the bentonite clay, it is unlikely that the pH at the overpack surface will be high enough to cause caustic cracking, even if an alkaline plume reaches the container.

Based on environmental considerations, the most likely forms of SCC are those in HCO_3^-/CO_3^{2-} environments. These forms of cracking have been observed on buried pipelines and are referred to as high-pH and low- (or near-neutral) pH SCC, based on the range of pH of the electrolyte found in contact with patches of SCC in the field (Parkins 2000). High-pH SCC is observed in concentrated HCO_3^-/CO_3^{2-} solutions (of the order of 0.1-1 mol·dm^{-3}) at pH 9.5-11.5 (Figure 22). Crack growth involves a film-rupture/anodic dissolution mechanism, requiring that the potential be in the range of the active/passive transition. Near-neutral pH SCC is associated with dilute (~0.01 mol·dm^{-3} HCO_3^-/CO_3^{2-}) solutions, a pH in the range pH 5.5-7.5, and potentials close to the open-circuit potential in anaerobic environments (Figure 22). A corrosion fatigue mechanism has been proposed (Been et al. 2004, 2005). It is significant that each form of SCC occurs at a pH corresponding to one of the pK's for the $H_2CO_3/HCO_3^-/CO_3^{2-}$ system (the H_2CO_3/HCO_3^- equilibrium in the case of near-neutral pH SCC and the HCO_3^-/CO_3^{2-} equilibrium for high-pH SCC).

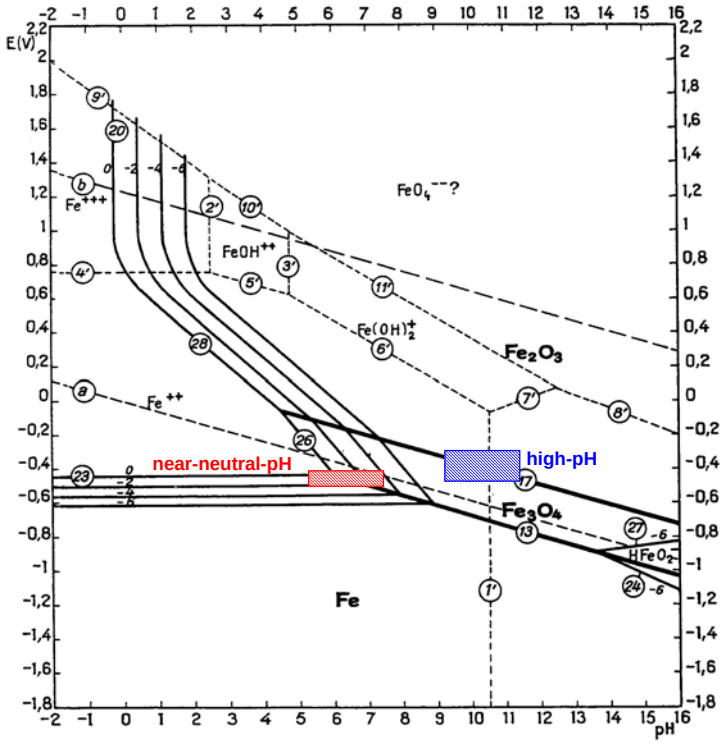


Figure 22: Potential-pH Diagram for Iron Showing the Regions of Susceptibility for the Two Forms of Stress Corrosion Cracking of C-steel Pipelines (King 2005a).

These forms of SCC are unlikely to affect a C-steel container in the repository. The high-pH environment is unlikely to form on the UFC surface because of the need for a highly concentrated HCO_3^-/CO_3^{2-} solution. Since the container surface temperature will likely not exceed 100°C, the only concentration mechanism that could generate such solutions involves the deliquescence of precipitated salts during the initial saturation of the repository. However, Cl^- salts tend to deliquesce at a higher temperature (or lower relative humidity) than carbonate salts, so it is unlikely that concentrated HCO_3^-/CO_3^{2-} solutions will form by deliquescence. The environment for near-neutral pH SCC is possible, however, and it is difficult to exclude this form of cracking on environmental grounds.

Loading and stresses

The presence of tensile stresses is required to cause SCC. A steel used fuel container may be subjected to tensile stresses resulting from the external pressure loads in a repository or from residual stresses resulting from the fabrication and closure welding processes.

In a repository, a container will be subjected to external monotonic pressure loads from hydrostatic pressure, bentonite swelling pressure, and lithostatic pressure (only from shale) (Maak 2006). Stresses will be induced into the container wall and lid by the external pressure load. Compressive stresses will be present on most of the external surface of the container, which will not induce SCC. However, relatively low tensile stresses (i.e., about 5% of the yield

strength of C-steel) will be present in a small area on the wall the container near the lid region (Saiedfar and Maak 2000). The containers are not subjected to any cyclic loading in a repository.

The strongest argument against the high-pH and low-pH forms of cracking is the need for cyclic loading for sustained crack growth (Parkins 2000). Near-neutral pH SCC is believed to be a form of corrosion fatigue, with cracks becoming dormant at low frequencies (Been et al. 2005). Cyclic loading may be necessary for high-pH for rupture of the film at the crack tip and the importance of cyclic softening (Parkins 2000). In both cases, sustained crack growth is highly unlikely for a monotonically loaded container in the repository. However, there is a need to confirm that SCC of steel containers will not be caused by static loading under expected repository conditions.

Residual stress could result in superficial cracking of the container. Figure 23 shows the cross section through a crack in pipeline steel typical of the vast majority of cracks found in the field. Approximately 99% of the cracks observed are of the order of 0.5-1 mm deep and exhibit rounded crack tips and corroded crack walls. These cracks are dormant and are believed to have stopped growing as the crack penetrated beyond the surficial layer of tensile residual stress. Although these cracks would not represent a threat to the integrity of the UFC, their formation should be avoided through post-weld stress relief of the final closure weld.

Residual stresses can result from the fabrication welding process of the C-steel container. However, suitable post-weld heat treatment (PWHT) at elevated temperature (i.e., > 600^{o}C) can be employed to remove the residual stresses from welding, which also soften the hardened microstructure in the heat-affected zone. During fabrication, PWHT can be freely carried out since there is no risk of damaging the used fuel.

For the final closure weld, PWHT at an elevated temperature is not recommended because of concerns over thermal damage to the used fuel. However, other types of stress-relief treatment could be considered. Figure 24 shows the beneficial effect of shot peening on the distribution of residual stress on pipeline steel (Eadie et al. 2002). A net compressive stress of ~500 MPa was induced at the surface, with some benefit to depths of ~0.6 mm. Machining of the final

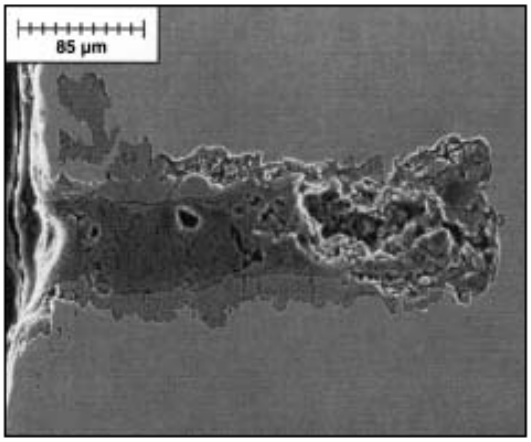


Figure 23: Cross-section of Dormant Crack in Pipeline Steel (Chen et al. 2002).

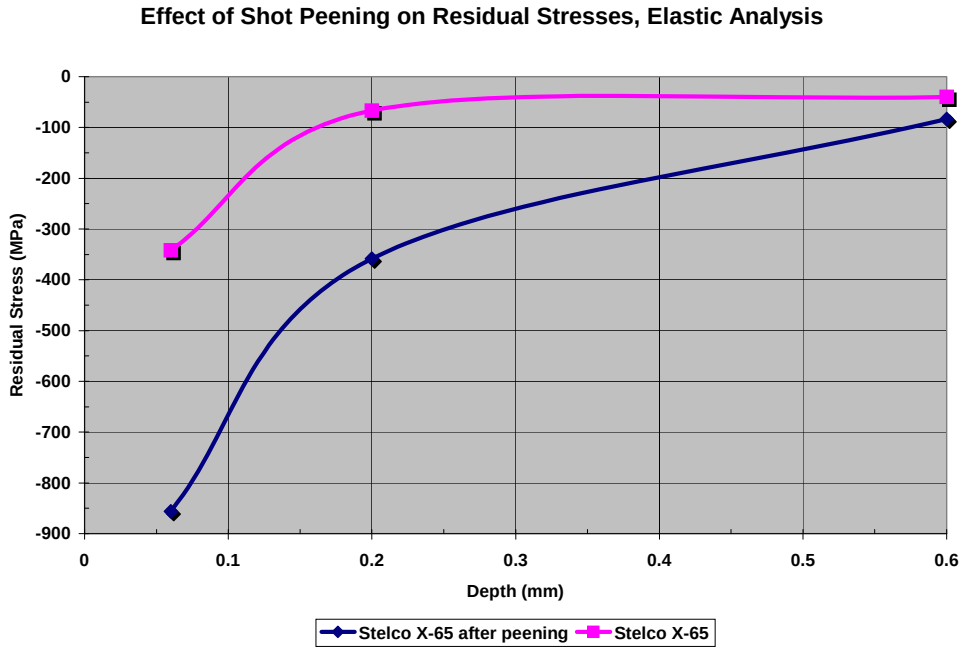


Figure 24: Effect of Shot Peening on the Distribution of Residual Stress on Pipeline Steels (Eadie et al. 2002).

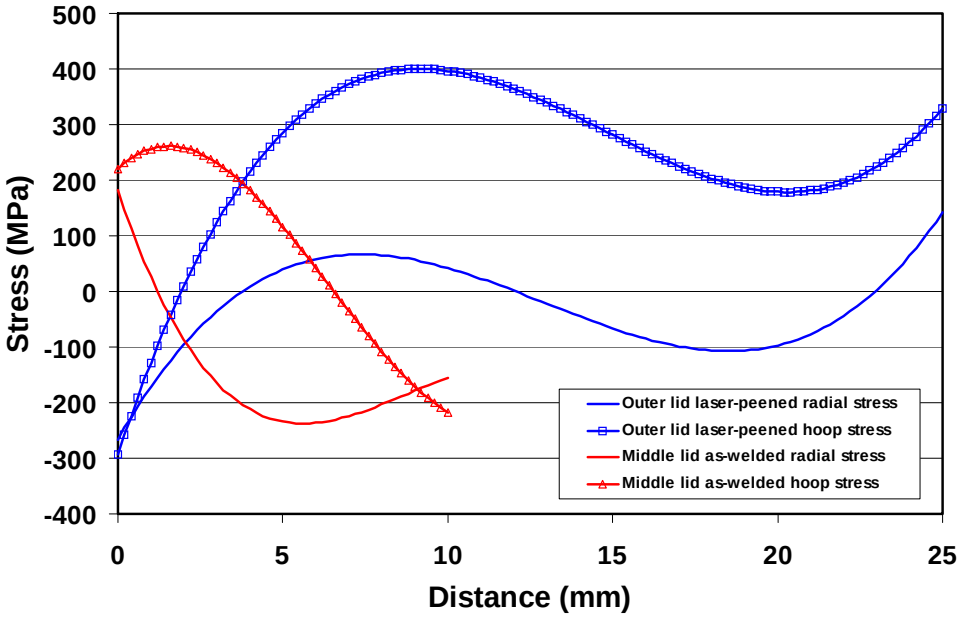


Figure 25: Depth Dependence of the Residual Stress in the Hoop and Radial Directions for the Laser-Peened Outer Closure Lid and the Middle Closure Lid Welds for an Alloy 22 Waste Package (after BSC 2004).

weld bead will also reduce the stress magnification resulting from the shape of the weld (Eadie et al. 2002). Laser peening is being considered as a post-weld stress-relief treatment in the U.S. Yucca Mountain Project. Figure 25 shows the magnitude of the reduction in residual tensile stress in Alloy 22 closure welds resulting from laser peening (BSC 2004). As with shot-peening, a net reduction in surface stress of ~500 MPa is possible which, in this case, was sufficient to produce a net surface compressive stress. Compressive stresses persisted for a depth of 2-4 mm in this case.

3.5 MICROBIOLOGICALLY INFLUENCED CORROSION

There are a number of forms of microbiologically influenced corrosion (MIC) of C-steel (Little et al. 1991). Microbiologically influenced corrosion of C-steel is most often associated with sulphate-reducing bacteria (SRB) and the formation of sulphide. However, there are others forms of MIC associated with acid-producing bacteria. In addition, any form of microbial activity that produces a biofilm can potentially induce localized corrosion.

The most aggressive forms of MIC occur underneath biofilms (Little et al. 1991). However, as for copper containers, biofilm formation on the surface of a steel container is not believed to be possible and only those remotely produced microbial metabolic by-products that could reach the container are considered here. Again, as for the MIC of Cu containers, the main threat is from hydrogen sulphide (HS^-) produced by SRB. Sulphide may enhance the rate of uniform corrosion although, depending on the flux of HS^-, the iron sulphide film that forms may be protective. Of greater concern, however, is the enhanced entry of H into the steel. Sulphide promotes H entry (King et al. 2005), leading to higher sub-surface hydrogen concentrations and increased possibility of HIC or blistering (see Section 3.3).

In order for the highly compacted bentonite (HCB) buffer material surrounding the UFC to minimize microbial activity, the following conditions of the HCB material will need to be met (Stroes-Gascoyne et al. 2006):

a) a water activity values below 0.96, or
b) a swelling pressure values at or above 2 MPa together with an in situ dry density of 1.6 $g \cdot cm^{-3}$ (i.e., an effective montmorillonite dry density of 1.4 $g \cdot cm^{-3}$) for a porewater salinity <100 $g \cdot dm^{-3}$, or
c) a pore-water salinity in excess of 100 $g \cdot dm^{-3}$.

As mentioned in Section 2, the groundwater and thus the equilibrated pore-water salinity in a DGR is expected to be in excess of 100 $g \cdot dm^{-3}$. The swelling pressure of the bentonite buffer would decrease with increasing pore-water salinity (Dixon 2000). Under expected sedimentary-rock DGR environments, the swelling pressure requirement (i.e., > 2 MPa) will not be met. However, microbial activity on or near the used-fuel container surface will be suppressed or prohibited by the presence of high groundwater and pore-water salinity (i..e., >100 $g \cdot dm^{-3}$) and the associated low water activity (i.e., <0.96).

3.6 CORROSION BEHAVIOUR OF WELDS

Sealing of the UFC will be accomplished by welding the closure lid to the body of the container. Welds are often preferential locations for corrosion and cracking to occur, and special attention must be paid to the design, fabrication, post-weld stress relief (if any), and inspection of the weld in order to ensure sufficient long-term integrity. At this stage, neither the material of construction nor the welding procedure have been defined for the Canadian repository program.

Weld development studies for C-steel containers have been performed in Japan (Asano and Aritomi 2005; Asano et al. 2005, 2006a,b). Tungsten inert gas (TIG) and electron beam (EB) welds have been produced in C-steel plates with a thickness of 40-190 mm, the upper end of the range corresponding to the proposed thickness of the C-steel overpack in the Japanese program. High quality TIG welds were produced, with no significant weld flaws (Asano et al. 2005). Electron-beam welding produced welds that were less satisfactory, primarily because of the surface protrusions and porosity at the start and end of the weld (Asano et al. 2006a), and it was concluded that further work was necessary. Weld porosity was also an issue for the EB welding of thick Cu canisters in the Swedish program (King 2004).

Residual stress measurements were also made on the completed welds. Tensile stress levels were lower for the EB welds (of the order of 200-300 MPa) than for the TIG welds (300-400 MPa), compared with the yield and ultimate strengths of the base material of 176-310 MPa and 378-430 MPa, respectively. For TIG welds, the maximum tensile residual stress was located at a depth of 10-20 mm below the surface and, in terms of the surface stress, at a distance of 15-30 mm away from the centre of the weld (Asano et al. 2005). For EB welds, the maximum tensile residual stress was located at a depth of ~30 mm and 30-50 mm away form the centre of the weld for the maximum surface tensile stress (Asano et al. 2006a). Post-weld stress relief through shot- or laser-peening (Figures 24-25) should be capable of imparting a net compressive residual stress on the closure weld without the need to heat the UFC and its contents.

A limited series of corrosion tests have been performed on the TIG and EB welds. Much of this work is only available in Japanese (Mitsui et al. 2005, 2006a-c), although a paper on the SCC susceptibility of C-steel welds in CO_3^{2-} is planned in 2007 (Y. Yokoyama, private communication 2007).

Corrosion tests of TIG, EB, and gas-metal arc welds (MAG) have been performed in aerobic synthetic seawater and a dilute groundwater solutions at 80^{o}C for a period of 90 days (Yokoyama et al. 2007). These environments were selected to represent the early transient conditions in the repository. Preferential attack of the weld metal was observed for TIG- and MAG-welded specimens, but no preferential attack occurred on EB-welded samples. Weight-losses were higher in the dilute groundwater, possibly because of the lower [O_2] in the synthetic seawater due to salting-out effects. Less corrosion was observed in synthetic seawater if bentonite was added to make a stiff slurry (solid:solution ratio 1 Mg:1 m^{-3}), again possibly because of mass-transport limitations on the supply of O_2 to the surface. Plans are in place for long-term (>1 year) immersion tests and for tests in anaerobic environments, as well as SCC testing.

Conventional arc welding processes for fabricating the steel container will result in the development of hardened microstructures in the heat-affected zone, which will be more

susceptible to SCC than the base metal. Elevated-temperature post-weld heat treatment can be used to temper and reduce the hardness of the heat-affect zone, which will also reduce residual stresses and the hydrogen content in the weld metal and heat-affected zone. However, if PWHT is not permitted due to the concern over thermal damage to the used fuel, the temper bead welding technique can be potentially used to produce a tempered heat-affected zone with acceptable hardness without the need for PWHT at high temperatures. Other types of stress relief processes can be used to reduce the residual stresses of the final closure weld.

Although still at a relatively early stage of development, there are indications that both high-quality and corrosion-resistant welds are possible for thick-walled C-steel containers.

3.7 OXIDATION OF CARBON STEEL

During the initial heating cycle immediately following placement of the UFC, the container surface will be dry and subject to dry air oxidation as opposed to aqueous corrosion processes. However, the rate of oxidation is small for temperatures ~100°C, the expected maximum UFC surface temperature. Stahl et al. (1995) have proposed the following expression for calculating the extent of dry air oxidation:

$$X = 1.787 \times 10^{5}\, t^{0.33} \exp(-6870/T) \tag{15}$$

where X is depth of metal lost through oxidation in time t (a) at temperature T (K). Differentiation of Equation (15) gives the following expression for the rate of oxidation:

$$\frac{dX}{dt} = 5.90 \times 10^{4}\, t^{-0.67} \exp\left(-\frac{6870}{T}\right) \tag{16}$$

For the UFC temperature profile given by King (2006), corresponding to a maximum surface temperature of 95°C attained at 10-30 years following placement, the cumulative extent of dry air oxidation over the first 1000 a is only 0.007 μm. This amount of corrosion is trivial in comparison to that resulting from aqueous corrosion processes and can be ignored in UFC lifetime assessments.

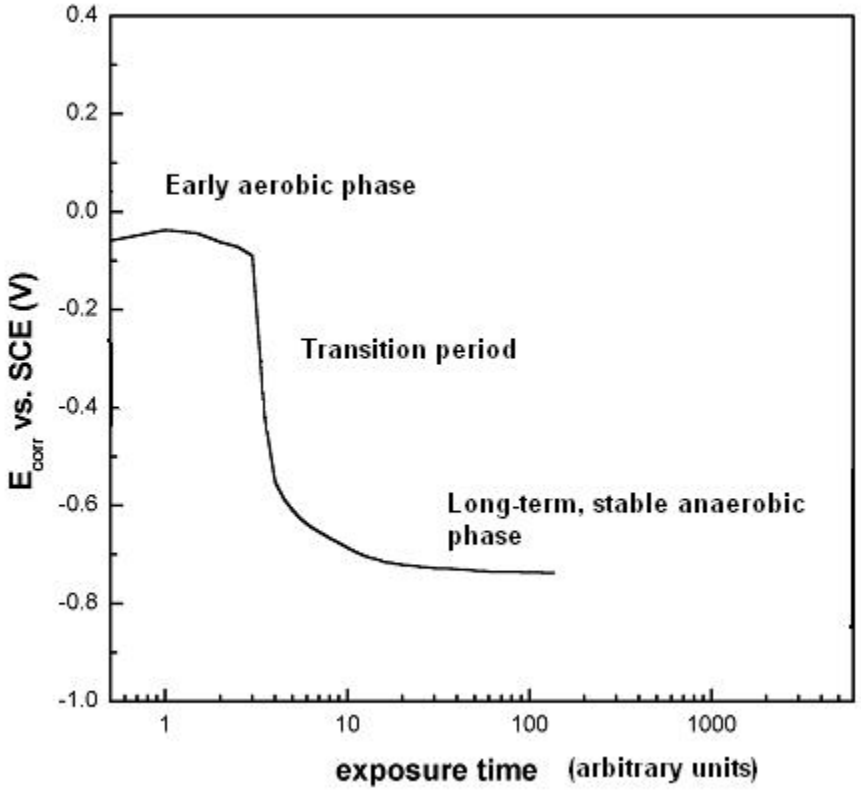


Figure 26: Schematic of Expected Evolution of the Corrosion Potential of a Carbon Steel Used Fuel Container in a Canadian Repository in Sedimentary Host Rock.

4. QUALITATIVE DESCRIPTION OF CORROSION BEHAVIOUR OF CARBON STEEL USED FUEL CONTAINERS

The preceding discussion of the various corrosion processes that might affect a C-steel UFC provides sufficient information to enable a qualitative description of the evolution of the corrosion behaviour of the container. For this purpose, it is convenient to divide the evolutionary timescale into three periods, namely:

1. the early aerobic phase,
2. the transition period between aerobic and anaerobic conditions, and
3. a long-term, stable anaerobic period.

Furthermore, it is also convenient to express the corrosion evolutionary path in terms of the time dependence of the corrosion potential of the container. Figure 26 shows a schematic illustration of how the E_{CORR} of a C-steel UFC might be expected to evolve over time in a Canadian DGR in a sedimentary host-rock formation.

Early aerobic phase

During the early aerobic phase, the following corrosion processes will occur:

- slow dry air oxidation as a result of dry-out of the UFC surface,
- the possible initiation of localized corrosion resulting from non-uniform wetting of the surface due to deliquescence of salt contaminants,
- loss of driving force for localized corrosion as surface progressively wets due to the increase in %RH and decrease in temperature,
- possible passivation of the UFC surface if the interfacial pH increases above the threshold of pH 8.5-10,
- localized breakdown of the passive film (if present) by Cl^- and/or SO_4^{2-} ions, counteracted by the protective effects of HCO_3^-/CO_3^-,
- propagation of localized corrosion (if initiated) due to separation of anodic and cathodic reactions,
- uniform corrosion of evenly wetted surfaces supported by the reduction of O_2,
- decreasing rate of uniform corrosion due to the development of a protective oxide film and the consumption of O_2,
- corrosion may occur under vapour phase or saturated conditions, depending upon the rate of saturation,
- progressive development of a roughened uniform corrosion front as opposed to localized corrosion in the form of pits or crevices,
- absence of H effects since corrosion supported by O_2 reduction, rather than the reduction of H_2O,
- absence of preferential weld corrosion due to proper weld design and welding procedures,
- absence of SCC due to the presence of compressive residual surface stress imparted by post-weld stress relief, and
- absence of MIC at the container surface because of either the low water activity or the eventual development of a bentonite swelling pressure.

The corrosion potential will be relatively positive during the early aerobic phase, once aqueous conditions have become established on the container surface (Figure 26). The presence of O_2, and the subsequent formation of Fe(III), will ensure potentials more positive than approximately –0.3 to –0.4 V_{SCE}. Such positive values may be sufficient to initiate localized corrosion if the surface is passive (Figure 17). As the O_2 is consumed, E_{CORR} will shift to progressively negative values.

Transition period between aerobic and anaerobic conditions

The transition from aerobic to anaerobic conditions will occur from a few 10's to a few 100's of years following placement of the containers. During this period, the repository may or may not be saturated by groundwater. Corrosion will be characterized by:

- continuing uniform and/or localized corrosion supported by reduction of the last traces of O_2,
- onset of uniform corrosion supported by the reduction of H_2O, and the concomitant generation of H_2,
- corrosion may occur under vapour phase or saturated conditions, depending upon the rate of saturation,

- reductive dissolution of Fe(III)-rich corrosion products formed during the aerobic phase, with possible initiation of localized corrosion by galvanic coupling of oxide reduction and C-steel dissolution,
- progression to uniform corrosion as pores in the corrosion product layer open up and as Fe(III) is progressively reduced to Fe(II),
- accumulation of expansive corrosion products at the surface, resulting in compaction of bentonite and increased load on the container,
- absorption of H by container material and, depending upon the degree of saturation of the near-field, the possible generation of a separate H_2 gas phase,
- absence of H effects through proper selection of the container material, ensuring that $c_H^0 < (c_H^0)_{TH}$,
- absence of preferential weld corrosion due to proper weld design and welding procedures,
- absence of SCC due to the presence of compressive residual surface stress imparted by post-weld stress relief, and
- absence of MIC at the container surface because of either the low water activity or the eventual development of a bentonite swelling pressure.

During the transition period, the E_{CORR} also goes through a transition from the relatively positive values characteristic of the aerobic phase to the more-negative values characteristic of anaerobic conditions (Figure 26). The rate at which E_{CORR} passes through this transient will depend on the quantity of Fe(III) corrosion products, the porosity of the surface layer, the rate of film (pore) dissolution, and the relative rates of Fe(III) and H_2O reduction. Potentially damaging localized corrosion can result if the transition period is slow and the potential is maintained in the –0.3 V_{SCE} to –0.6 V_{SCE} range for an extended period of time.

Long-term, stable anaerobic period

Eventually, the environment will evolve to a stable, long-term anaerobic condition characterized by the absence of O_2 and fully saturated near-field. Under these conditions, the expected corrosion behaviour is as follows:

- slow uniform corrosion supported by the reduction of H_2O,
- the absence of localized corrosion,
- progressive reduction in the degree of surface roughening,
- continued accumulation of H_2 at the container surface and its transport into the near- and far-fields,
- absence of H effects through proper selection of the container material, ensuring that $c_H^0 < (c_H^0)_{TH}$,
- absence of preferential weld corrosion due to proper weld design and welding procedures,
- accumulation of expansive corrosion products at the surface, resulting in compaction of bentonite and increased load on the container,
- gradual loss of the surface layer of compressive residual stress by corrosion,
- absence of SCC because of a combination of an unsupportive environment and/or the absence of cyclic loading,
- absence of MIC at the container surface because of either the low water activity or the bentonite swelling pressure,

- eventual UFC failure as the wall thins to below the thickness required to sustain the external load from hydrostatic and buffer swelling pressures and the load from expansive corrosion products.

The anaerobic phase is characterized by a stable E_{CORR} value in the range –0.7 V_{SCE} to -0.8 V_{SCE} (Figure 26).

5. CARBON STEEL CONTAINER FAILURE MODEL

5.1 TREATMENT OF CORROSION PROCESSES

The conceptual C-steel UFC failure model is relatively simple since many of the possible corrosion processes of concern can be excluded based on either the expected environmental conditions in a deep geological repository or by proper container design and fabrication. Only two corrosion processes need to be quantitatively assessed in order to predict container lifetimes: uniform corrosion and the degree of localized attack. All other corrosion processes, including H effects, SCC, MIC, preferential weld attack, and dry air oxidation, can be excluded from consideration in the repository.

5.1.1 Uniform Corrosion

The extent of uniform corrosion should be assessed through a combination of (i) mass-balance arguments in the case of aerobic conditions, (ii) empirical corrosion rate data for the anaerobic phase, and (iii) a mechanistic mixed-potential model to provide support and justification for the calculations of the rate of wall loss. This combination of calculations and mechanistic modelling provides a justifiable, robust prediction of the long-term uniform corrosion behaviour of a C-steel UFC.

The calculation of the maximum extent of uniform corrosion during the aerobic phase is trivial. The volume of trapped O_2 in the pores of the as-placed buffer and backfill sealing materials is normalized with respect to the affected containers. Deep geological repositories typically contain 1-10 $mol_{O2} \cdot m^{-2}$ of container surface area. If all of this O_2 resulted in uniform corrosion of the container, the resulting wall loss would be of the order of 10-100 μm. Various “what-if” scenarios can be assessed for scenarios in which the O_2 might only affect a certain fraction of the container surface, for example, as a result of uneven saturation of the bentonite.

For anaerobic corrosion, it is common to assume a constant corrosion rate (Johnson and King 2003, King 2005a). Whether the rate is constant, and what that rate should be, can be determined from existing information in the literature or from new, targeted, experiments. Both long-term laboratory and archaeological evidence suggests that the anaerobic corrosion rate is in the range 1-10 $\mu m \cdot a^{-1}$. What is missing, however, is the supporting mechanistic argument for whether this rate is constant or whether it continues to decrease with time. In addition, the effects of pore-water and groundwater constituents, such as HCO_3^-/CO_3^{2-} and Cl^-, are not well understood at this time.

A mixed-potential model for C-steel UFC is required to support the predictions of uniform corrosion during the aerobic and anaerobic phases. There is a significant electrochemical database available to support such a model, although additional data may be needed on the

kinetics of H_2O reduction. In addition, the effects of film formation on E_{CORR} need further investigation. However, as noted below, such a model will not only support the uniform corrosion predictions, but will also allow a more-rigorous assessment of the likelihood of localized corrosion.

5.1.2 Localized (Pitting) Corrosion

As proposed above for uniform corrosion, the effect of localized corrosion on the lifetime of C-steel containers should be assessed through a combination of empirical data and mechanistic modelling. The empirical data are used to estimate the time-dependence of the degree of localization, whereas the mechanistic modelling is used to justify these long-term predictions.

Empirical localized corrosion data for C-steel currently exist, for example, as shown in Figure 19. These data should be supplemented by additional data from the literature, most notably the large database available from the pipeline industry. The current data format, i.e., pitting factor as a function of the mean depth of corrosion, is suitable for predictive modelling, since the depth of uniform corrosion can be calculated as described above.

As for uniform corrosion, mechanistic modelling is used to support the empirical calculations of localized corrosion damage. Mechanistic descriptions are required for each of the postulated localized corrosion scenarios. The mixed-potential model described above is suitable for predicting whether localized corrosion due to breakdown of a passive film is possible (and, indeed, whether a passive film will form in the first place), and the possibility and duration of localized corrosion due to coupling of oxide reduction and C-steel dissolution during the transition from aerobic to anaerobic conditions. A modified model will be required to assess the extent of localized corrosion due to non-uniform wetting of the surface during the early stages of the aerobic phase.

Additional localized corrosion scenarios, for example, the dissolution of steel coupled to enhanced H_2O reduction on Fe_3O_4 surfaces, require mechanistic experimental verification.

5.1.3 Hydrogen Effects

Numerical assessment of H-related effects is specifically excluded from the conceptual C-steel UFC failure model. As described in detail above, it is assumed that the material of construction will be specified in order to minimize the possibility of HIC or blister formation. In addition, existing experimental evidence suggests that the sub-surface H concentration is less than the threshold for H damage, even for vintage ferrite-pearlite steels. Therefore, the avoidance of H-related failure mechanisms is a credible UFC design criterion.

5.1.4 Stress Corrosion Cracking

As with H-related effects, the possibility of SCC of the C-steel container is specifically excluded from the UFC failure model. Stress corrosion cracking can be excluded from consideration based on a combination of environmental- and stress-related arguments. Aggressive environments, except possibly that associated with near-neutral pH SCC, are unlikely to be generated in the repository. The necessary stress, either in the form of cyclic loading or a

tensile residual stress, will also be absent, either because of the nature of the environment or, in the case of residual stress, because of suitable post-weld stress relief.

It is possible that near-neutral pH SCC cracks could initiate once the near-surface region of tensile residual stress has been corroded. However, although cracks might initiate in the then-exposed tensile residual stress layer, propagation to failure will not occur because of the absence of cyclic loading that has been shown to be necessary for crack growth for this form of SCC.

5.1.5 Microbiologically Influenced Corrosion

Microbiologically influenced corrosion is not currently accounted for in the C-steel lifetime assessment. As previously argued for Cu UFC, the near-field environment will not support microbial activity or biofilm formation on the container surface. Therefore, the only possible cause of MIC is the transport of corrosive metabolic by-products produced in less-inhospitable regions of the repository to the container surface. Analyses performed to date (King et al. 2004) show that the amount of sulphide that could reach the container surface due to remote SRB activity is minimal.

Therefore, no allowance is currently included for MIC in C-steel UFC lifetime predictions.

5.1.6 Welds

Preferential weld corrosion can be avoided by proper weld design and welding procedures. Recent Japanese evidence suggests that non-susceptible weld material can be produced using existing techniques (Yokoyama et al. 2007). Therefore, no allowance is made in the current conceptual model for preferential attack at welds in the C-steel UFC.

In lifetime assessments in the Japanese program, only a fraction of the wall thickness is used as a corrosion allowance (Asano and Aritomi 2005). This reduction in wall thickness is partly from concerns about the ability of inspection techniques to detect deep sub-surface weld flaws. Depending upon future developments in inspection techniques and the ability to detect sub-surface weld flaws remotely, it may be necessary to use a corrosion allowance for the C-steel UFC that is less than the wall thickness.

5.1.7 Oxidation

The extent of dry air oxidation during the initial dry-out period has been shown above to be trivial and is not included in the C-steel UFC lifetime assessment.

5.2 CONTAINER FAILURE

5.2.1 Mechanical Overload

Final failure of a UFC is unlikely to result from complete corrosion of the container wall resulting in ultimate perforation. Instead, failure will result from mechanical overload, as the reduced wall thickness becomes unable to support the external load exerted by the combination of (i) hydrostatic pressure, (ii) bentonite swelling pressure, (iii) the pressure of H_2 gas, and (iv) forces from the formation of expansive corrosion products.

The point at which the UFC would fail mechanically is not currently known, and needs to be assessed using a combined corrosion-structural model.

5.2.2 Time Dependence of Failure Aperture

At the time of container penetration, the entire surface of the UFC does not disappear. The failed container is expected to continue to provide significant mass-transport resistance, first to the diffusion of H_2O into the container and then to the diffusion of released radionuclides into the near-field. Depending upon the mean remaining wall thickness at the time of container failure, there may be some benefit in taking credit for the continued barrier function offered by the remaining wall.

5.2.3 Preliminary Lifetime Assessment

Preliminary corrosion assessments have been performed for a C-steel container in a repository in Michigan Basin sedimentary formations (King 2005a). Based on a combination of uniform and pitting corrosion, the range of wall penetrations was estimated to be 9-34 mm after 10,000 years (1-10 mm as uniform corrosion and 8-24 mm as pitting) and 34-175 mm after 100,000 years (10-100 mm as uniform corrosion and 24-75 mm as pitting).

No structural analysis has been performed to estimate the remaining wall thickness of a steel container necessary to provide mechanical integrity in a DGR in sedimentary rock. In order to withstand the external pressure loads in a DGR in sedimentary rock, it is expected that a steel container would need a wall thickness of the order of 100 mm, which is similar to the wall thickness of the inner steel vessel of the reference copper used-fuel container (Maak 2006, Saiedfar and Maak 2000, Maak and Simmons 2001). The container thickness will be determined based on structural analyses that will follow the intent of the ASME Boiler and Pressure Vessel Code with a safety factor of 3 for the pre-glaciation period (10,000 years is considered to be within the pre-glaciation period). This means that a steel container with a remaining thickness of about 66 mm (100 mm minus the 34 mm maximum corrosion penetration) should still have adequate mechanical strength with a substantial safety margin to withstand the external pressure for a period of at least 10,000 years. No container failure or full-wall penetration is expected and a steel container should still be capable of providing containment of the used fuel for a period of more than 10,000 years after it is placed in a repository.

A summary of this, and other earlier, lifetime predictions for C-steel containers is given in Table 1 (King 2005a).

6. CONCLUSIONS

A conceptual model for the corrosion of a C-steel used fuel container in a deep geological repository in sedimentary rock has been described. The model takes into account various corrosion processes that might affect the container in the repository environment. Some processes, such as uniform corrosion and localized attack, are specifically included in the calculation of the container lifetime. Other processes, such as H-related effects, stress corrosion cracking, microbiologically influenced corrosion, preferential weld corrosion, and dry air oxidation are currently excluded from the assessment. This is based on the assumptions that the environment will either not support these processes or that these corrosion mechanisms can be avoided by proper container design and fabrication processes.

The validity of these assumptions will need to be examined in the future through more-detailed engineering assessment, mathematical modelling, and experimental studies.

The extent of uniform corrosion should be assessed through a combination of (i) mass-balance arguments in the case of aerobic conditions, (ii) empirical corrosion rate data for the anaerobic phase, and (iii) a mechanistic mixed-potential model to provide support and justification for the calculations of the rate of wall loss. This combination of empirical calculations and mechanistic modelling provides a justifiable, robust prediction of the long-term uniform corrosion behaviour of a C-steel UFC.

Similarly, the effect of localized (pitting) corrosion on the lifetime of C-steel containers should be assessed through a combination of empirical data and mechanistic modelling. The empirical data are used to estimate the time-dependence of the degree of localization, whereas the mechanistic modelling is used to justify these long-term predictions.

Preliminary C-steel container lifetime assessments suggest that, based on a combination of uniform and localized (pitting) corrosion, the range of wall penetration is 9-34 mm after 10,000 years and 34-175 mm after 100,000 years. A 100-mm-thick C-steel container with a reduction in wall thickness of 34 mm is still expected to have adequate mechanical strength and no container failure of through-wall penetration is expected. This analysis suggests, therefore, that C-steel containers can provide containment of used nuclear fuel for a period of more than 10,000 years after being placed in a deep geological repository in sedimentary rock.

ACKNOWLEDGEMENT

The author would like to acknowledge useful review comments and suggestions for improvements from Peter Maak and Sean Russell, NWMO.

REFERENCES

Andra. 2005. Dossier 2005 Argile. Andra (Châtenay-Malabry, France, December 2005).

Asano, H. and M. Aritomi. 2005. Long-term integrity of waste package final closure for HLW geological disposal, (I) Points at issue concerning 1,000 years containment capability of overpack. J. Nucl. Sci. Technol. 42, 470-479.

Asano, H., S. Sawa, and M. Aritomi. 2005. Long-term integrity of waste package final closure for HLW geological disposal, (II) Applicability of TIG welding method to overpack final closure. J. Nucl. Sci. Technol. 42, 573-587.

Asano, H., K. Maeda, and M. Aritomi. 2006a. Long-term integrity of waste package final closure for HLW geological disposal, (III) Applicability of electron beam welding to overpack final closure. J. Nucl. Sci. Technol. 43, 206-221.

Asano, H., S. Kataoka, K. Maeda, and M. Aritomi. 2006b. Long-term integrity of waste package final closure for HLW geological disposal, (IV) Influence of welding and prediction of long-term integrity of weld joint. J. Nucl. Sci. Technol. 43, 924-936.

Ashley, G.W. and G.T. Burstein. 1991. Initial stages of the anodic oxidation of iron in chloride solutions. Corrosion 47, 908-916.

ASM. 1987. Corrosion of carbon steels. In Metals Handbook, Ninth edition, Volume 13, Corrosion. American Society for Metals International, Metals Park, OH, pp. 509-530.

Been, J., H. Lu, R. Eadie, G. Shen, R. Sutherby. 2004. The role of stress intensifiers in near-neutral pH corrosion fatigue of line pipe. In Proc. CORROSION/2004, NACE International (Houston, TX), Paper no. 04552.

Been, J., F. King, and R. Sutherby. 2005. Environmentally assisted cracking of pipeline steels in near-neutral pH environments. In Proc. Second International Conference on Environment-Induced Cracking of Metals (EICM-2), Banff, AB, September 20-23, 2004 (Elsevier), in press.

Bel, J.J.P., S.M. Wickham, and R.M.F. Gens. 2006. Development of the *Supercontainer* design for deep geological disposal of high-level heat emitting radioactive waste in Belgium. In Scientific Basis for Nuclear Waste Management XXIX, (P. Van Iseghem, Editor), Mat. Res. Soc. Symp. Proc. 932, Materials Research Society, (Warrendale, PA), 23-32.

Bird, H.E.H., B.R. Pearson, and P.A. Brook. 1988. The breakdown of passive films on iron. Corros. Sci. 28, 81-86.

Bockris, J.O'M. and A.N. Reddy. 1970. Modern Electrochemistry. Vol. 2. Plenum Press, New York.

Brossia, C.S. and G.A. Cragnolino. 2000. Effect of environmental variables on localized corrosion of carbon steel. Corrosion 56, 505-514.

BSC. 2004. Stress corrosion cracking of the drip shield, the waste package outer barrier, and the stainless steel structural material. Bechtel SAIC Company report to DOE, ANL-EBS-MD-000005 Rev 02, October 2004.

Calvo, E.J. and D.J. Schiffrin. 1988. The electrochemical reduction of oxygen on passive iron in alkaline solutions. J. Electroanal. Chem. 243, 171-185.

Chen, W., F. King, and E. D. Vokes. 2002. Characteristics of near neutral pH stress corrosion cracks in an X-65 pipeline steel. Corrosion 58, 267-275.

Chin, R.J. and K. Nobe. 1977. Effect of oxygen and benzotriazole on the corrosion characteristics of rotating iron disk electrodes in acidic chloride solutions. Corrosion 33, 364-369.

Ciaraldi, S.W. 1992. Stress-corrosion cracking of carbon and low-alloy steels (yield strengths less than 1241 MPa), in Stress-Corrosion Cracking Materials Performance and Evaluation, R.H. Jones (ed.). ASM International (Metals Park, OH), chap. 2.

Craig, B. 1987. Hydrogen damage, in Metals Handbook, 9th Edition. Volume 13 Corrosion. ASM International (Metals Park, OH), pp. 163-171.

Crossland, I. 2005. Long term corrosion of iron and copper. In ICEM'05: 10th International Conference on Environmental Remediation and Radioactive Waste Management, September 4-8, 2005 (American Society of Mechanical Engineers, New York, NY), paper ICEM05-1272.

Debruyn, W. 1990. Corrosion of container materials under clay repository conditions. In: Proceedings of Workshop on Corrosion of Nuclear Fuel Waste Containers, 1988, February 9 - 10. Winnipeg, MB. (D.W. Shoesmith, Editor). Atomic Energy of Canada Limited Report, AECL-10121, 1990, 175-186.

Debruyn, W., J. Dresselaers, Ph. Vermieren, J. Kelchtermans and H. Tas. 1991. Corrosion of container and infrastructure materials under clay repository conditions. Commission of the European Communities Report, EUR 13667 EN.

DECHEMA. 1990. Corrosion Handbook: Corrosive Agents and their Interaction with Materials, Volume 7, Atmosphere.

Dixon, D.A. 2000. Porewater salinity and the development of swelling pressure in bentonite-based buffer and backfill materials. Nagra Technical Report 00-04.

Eadie, R., L.W. Hunt, R. Sutherby, G. Roy, G. Shen, J. Luo, W. Chen, T.C. Hamré, F. King and T. Jack. 2002. Long seam welds in gas and liquids pipelines and near-neutral pH stress corrosion cracking. In Proc. International Pipeline Conf. 2002 (ASME International, New York, NY), paper 27118, 1629-1634.

Fukuda, T. and M. Akashi. 1995. Effect of [HCO_3^- + CO_3^{2-}] on corrosion crevice repassivation potential of carbon steel in simulated bentonite environment. In Scientific Basis for Nuclear Waste Management XIX, (W. Murphy and D.A. Knecht, Editors), Mat. Res. Soc. Symp. Proc. 412, Materials Research Society, (Pittsburgh, PA), 597-602.

Fukuda, T., M. Akashi and R.W. Staehle. 1995. The critical condition for the long range stability of electrochemical cells in carbon steel used for nuclear waste overpacks, Proc. of International Symposium on Plant Aging and Life Predictions of Corrodible Structures, pp.229-236.

Gervasio, D., I. Song, and J.H. Payer. 1998. Determination of the oxygen reduction products on ASTM A516 steel during cathodic reduction. J. Appl. Electrochem. 28, 979-992.

Gierszewski, P., J. Avis, N. Calder, A. D'Andrea, F. Garisto, C. Kitson, T. Melnyk, K. Wei and L. Wojciechowski. 2004. Third Case Study - Postclosure Safety Assessment. Ontario Power Generation, Nuclear Waste Management Division Report 06819-REP-01200-10109-R00. Toronto, Canada.

Gojkovic, S.Lj., S.K. Zecevic, and D.M. Drazic. 1994. Oxygen reduction on iron – part VI. Processes in alkaline solutions. Electrochimica Acta 39, 975-982

Golder. 2003. LLW geotechnical feasibility study Western Waste Management Facility, Bruce Site, Tiverton, Ontario. Golder Associates report to Ontario Power Generation, Report 021-1570.

Gordon, G.M. 2002. Considerations related to permanent disposal of high-level radioactive waste. Corrosion 58, 811-825.

Hay, M. 2003. Hydrogen-induced cracking in low strength steel. Short Course, COM'2003, Vancouver, August 2003.

Honda, A., T. Teshima, K. Tsurudome, H. Ishikawa, Y. Yusa and N. Sasaki. 1991. Effect of compacted bentonite on the corrosion behaviour of carbon steel as geological isolation overpack material. Materials Research Society Symposium Proceedings 212 (Materials Research Society, Pittsburgh, PA), pp. 287-294.

Jack, T.R., F. King, L. Yang, and R. Sutherby. 2003. Kinetic isotope effects in the corrosion and hydrogen loading of line pipe steel: implications for stress corrosion cracking. In Proc. Environmental Degradation of Materials & Corrosion Control in Metals (EDMCCM), J. Luo, M. Elboujdaini, D. Shoesmith, and P.C. Patnaik (eds.) (Canadian Institute if Mining, Metallurgy and Petroleum, Montreal, PQ), pp. 205-216.

JNC. 2000. H12: Project to establish the scientific and technical basis for HLW disposal in Japan. Japan Nuclear Cycle Development Institute, Supporting Report 2, Repository Design and Engineering Technology.

Johnson, L.H. and F. King. 2003. Canister options for the disposal of spent fuel. Nagra Technical Report 02-11.

Jovancicevic, V. and J.O'M. Bockris. 1986. The mechanism of oxygen reduction on iron in neutral solutions. J. Electrochem. Soc. 133, 1797-1807.

Kaesche, H. 1985. Metallic Corrosion. Principles of Physical Chemistry and Current Problems. Translated by R.A. Rapp. National Association of Corrosion Engineers, Houston, TX.

Katano, Y., K. Miyata, H. Shimizu, and T. Isogai. 2003. Predictive model for pit growth on underground pipes. Corrosion 59, 155-161.

King, F. 2002. Corrosion of copper in alkaline chloride environments. Swedish Nuclear Fuel and Waste Management Company Report, TR-02-5.

King, F. 2004. The effect of discontinuities on the corrosion behaviour of copper containers. Swedish Nuclear Fuel and Waste Management Company Report, TR-04-05.

King, F. 2005a. The corrosion behaviour of copper and steel containers in a deep geological repository in sedimentary rocks of the Michigan Basin. Ontario Power Generation, Nuclear Waste Management Division Report 06819-REP-01300-10101-R00.

King, F. 2005b. Evolution of environmental conditions in a deep geological repository in the sedimentary rock of the Michigan Basin, Ontario. Ontario Power Generation Nuclear Waste Management Division Report 06819-REP-01300-10102-R00.

King, F. 2006. Review and gap analysis of the corrosion of copper containers under unsaturated conditions. Ontario Power Generation, Nuclear Waste Management Division Report 06819-REP-01300-10124-R00.

King, F. and M. Kolar. 1999. Prediction of the effects of α-radiolysis, precipitation and redox reactions with Fe and Fe(II) on the dissolution of UO_2 using the mixed-potential model of fuel dissolution (MPM Version 1.1). Ontario Power Generation Nuclear Waste Management Division Report No: 06819-REP-01200-10014.

King, F. and M. Kolar. 2000. The copper container corrosion model used in AECL's second case study. Ontario Power Generation, Nuclear Waste Management Division Report 06819-REP-01200-10041-R00.

King, F. and M. Kolar. 2001. An improved C-steel corrosion model for the mixed-potential model for used fuel dissolution (MPM Version 1.4). Ontario Power Generation Nuclear Waste Management Division Report No: 06819-REP-01300-10027.

King, F. and M. Kolar. 2006. EPRI's Engineered Barrier System Corrosion Model (EBSCOM). In Proc. 11th International High-level Radioactive Waste Management Conference, American Nuclear Society (La Grange Park, IL), pps. 478-485.

King, F. and S. Stroes-Gascoyne. 1995. Microbially influenced corrosion of nuclear fuel waste disposal containers. In Proceedings 1995 International Conference on Microbially Influenced Corrosion, NACE International, Houston, TX, paper 35.

King, F. and S. Stroes-Gascoyne. 1997. Predicting the effects of microbial activity on the corrosion of copper nuclear waste disposal containers, in Microbial Degradation Processes in Radioactive Waste repository and in Nuclear Fuel Storage Areas, J.H. Wolfram (ed.), Kluwer Press, Dordrecht, p. 149-162.

King, F. and S. Stroes-Gascoyne. 2000. An assessment of the long-term corrosion behaviour of C-steel and the impact on the redox conditions inside a nuclear fuel waste disposal container. Ontario Power Generation Nuclear Waste Management Division Report No: 06819-REP-01200-10028.

King, F., M. Kolar and D.W. Shoesmith. 1996. Modelling the effects of porous and semi-permeable layers on corrosion processes. CORROSION/96, NACE International, Houston, TX, paper no. 380.

King, F., L. Ahonen, C. Taxén, U. Vuorinen and L. Werme. 2001. Copper corrosion under expected conditions in a deep geologic repository. Swedish Nuclear Fuel and Waste Management Company Report, SKB TR 01-23.

King, F., L. Ahonen, C. Taxén, U. Vuorinen, and L. Werme. 2002. Copper corrosion under expected conditions in a deep geologic repository. Posiva Oy Report POSIVA 2002-01.

King, F., M. Kolar, S. Stroes-Gascoyne, and P. Maak. 2004. Model for the microbiological corrosion of copper containers in a deep geologic repository. In Scientific Basis for Nuclear Waste Management XXVII, (V.M. Oversby and L.O. Werme, Editors), Mat. Res. Soc. Symp. Proc. 807, Materials Research Society, (Warrendale, PA), 811-816.

King, F., J. Been, and L. Yang. 2005. The effects of bicarbonate, chloride, sulphate and CO_2 on pitting, crack initiation and propagation of low-pH SCC. Gas Research Institute Final Report (Gas Technology Institute, Des Plaines, IL), GRI-04/0096.

Kolar, M. and F. King. 1996. Modelling the consumption of oxygen by container corrosion and reaction with Fe(II). Mats. Res. Soc. Symp. Proc. Vol. 412, Materials Research Society, Pittsburgh, PA, p. 547-554.

Kreis, P. 1991. Hydrogen evolution from corrosion of iron and steel in low/intermediate level waste repositories. Technical Report NTB 91-21, NAGRA, Winterthur, Switzerland.

Lanza, F. and C. Ronsecco. 1986. Corrosion of low-carbon steel in clay and sea sediments. Commission of the European Communities Report EUR 10522 EN.

Little, B., P. Wagner and F. Mansfeld. 1991. Microbiologically influenced corrosion of metals and alloys. Int. Mater. Rev. 36, 253-272.

Maak, P. 1999. The selection of a corrosion-barrier primary material for used-fuel disposal containers. Ontario Power Generation, Nuclear Waste Management Division Report 06819-REP-01200-10020-R00.

Maak, P. 2006. Used fuel container requirements. Ontario Power Generation Preliminary Design Requirements. 06819-PDR-01110-10000 R02.

Maak, P. and G.R. Simmons. 2001. Summary report: A screening study of used-fuel container geometric designes and emplacment methods for a deep geoloci repository. Ontario Power Generation, Nuclear Waste Management Division Report 06819-REP-01200-10065-R00.

MacFarlane, D.R. and S.I. Smedley. 1986. The dissolution mechanism of iron in chloride solutions. J. Electrochem. Soc. 133, 2240-2244.

Makar, G.L. and D. Tromans. 1996. Pitting corrosion of iron in weakly alkaline chloride solutions. Corrosion 52, 250-261.

Marschall, P., S. Horseman, and T. Gimmi. 2005. Characterisation of gas transport properties of the Opalinus Clay, a potential host rock formation for radioactive waste disposal. Oil & Gas Sci. Technol. – Rev IFP 60, 121-139.

Marsh, G.P. and K.J. Taylor. 1988. An assessment of carbon steel containers for radioactive waste disposal. Corrosion Science 28, 289-320.

Marsh, G.P., K.J. Taylor, S.M. Sharland, and P.W. Tasker. 1987. An approach for evaluating the general and localized corrosion of carbon-steel containers for nuclear waste disposal. Mat. Res. Soc. Symp. Proc. Vol. 84, Materials Research Society, Pittsburgh, PA, p. 227-238.

Marsh, G.P., A.H. Harker, and K.J. Taylor. 1989. Corrosion of carbon steel nuclear waste containers in marine sediment. Corrosion 45, 579-589.

Martinsek, A.T. 2003. Reliable inferences for the maximum pit depth within pitting colonies on long pipelines. Corrosion 59, 1058-1063.

Mazurek, M. 2004. Long-term used nuclear fuel waste management – geoscientific review of the sedimentary sequence in southern Ontario. Nuclear Waste Management Office Background Paper 6-12.

Miller, W.M., W.R. Alexander, N.A. Chapman, I.G. McKinley, and J.A.T. Smellie. 1994. Natural analogue studies in the geological disposal of radioactive wastes; Studies in Environmental Sciences 57, Elsevier, Amsterdam (also Nagra Technical Report NTB 93-03).

Mitsui, H., A. Otsuki, H. Asano, et al. 2005. In Proc. 52nd Japan Conf. on Materials and Environments, B-309, 249-252 [in Japanese].

Mitsui, H., A. Otsuki, H. Asano, et al. 2006a. In Proc. 53rd Japan Conf. on Materials and Environments, B-105, 127-130 [in Japanese].

Mitsui, H., N. Taniguchi, et al. 2006b. Study on the corrosion assessment of overpack welds-II. RWMC-JRJ-05001, JAEA-Research 2006-031 [in Japanese].

Mitsui, H., R. Takahashi, N. Taniguchi, et al.. 2006c. Study on the Corrosion Assessment of Overpack Welds-III. RWMC-JRJ-06001, JAEA-Research 2006-080 [in Japanese].

Miyata, Y. and S. Asakura. 2002. Oxygen reduction reaction at rust free iron surface in neutral unbuffered chloride solutions. Corrosion Science 44, 589-602.

Motamedi. M. 1999. The survival and activity of bacteria in compacted bentonite clay in conditions relevant to high level radioactive waste (HLW) repositories. Ph. D. Thesis. Department of Cell and Molecular Biology, Microbiology, Goteborg University, Sweden.

Nagra. 2002. Project Opalinus Clay. Safety Report. Nagra Technical Report NTB 02-05.

Nagra. 2004. Effects of post-disposal gas generation in a repository for spent fuel, high-level waste and long-lived intermediate level waste sited in Opalinus Clay. Nagra Technical Report NTB 04-06.

NWMO. 2005. Choosing a way forward. The future management of Canada's used nuclear fuel. Final study. Nuclear Waste Management Organization, Toronto, Ontario.

ONDRAF-NIRAS. 2002. Safety assessment and interim report 2. ONDRAF Report Ref: NIROND 2001-05.

Parkins, R.N. 2000. A review of stress corrosion cracking of high pressure gas pipelines. CORROSION/2000, National Association of Corrosion Engineers (Houston, TX), Paper No. 363.

Peat, R. S. Brabon, P.A.H. Fennell, A.P. Rance, and N.R. Smart.. 2001. Investigation of Eh, pH and corrosion potential of steel in anoxic groundwater. SKB Technical Report TR-01-01.

Pedersen K. 2000. Microbial processes in radioactive waste disposal. Swedish Nuclear Fuel and Waste Management Company Report, SKB TR 00-04.

Pedersen, K., M. Motamedi, O. Karnland and T. Sandén. 2000. Mixing and sulphate-reducing activity of bacteria in swelling, compacted bentonite clay under high-level radioactive waste repository conditions. J. Appl. Microbiol. 89, 1038-1047.

Pourbaix, M. 1974. Atlas of Electrochemical Equilibria in Aqueous Solutions, 2nd. edition. NACE International, Houston, TX.

Qin, Z., B. Demko, J. Noël, D. Shoesmith, F. King, R. Worthingham and K. Keith. 2004. Localized dissolution of millscale-covered pipeline steel surfaces. Corrosion 60, 906-914.

Romanoff, M. 1989. Underground Corrosion. NACE International, Houston, TX.

Russell, S.B. and G.R. Simmons. 2003. Engineered barrier system for a deep geological repository in Canada. In Proc. 10th Int. High-Level Radioactive Waste Management Conf., Las Vegas, NV, March 30-April 2, 2003 (American Nuclear Society, La Grange Park, IL), pp. 563-570.

Saiedfar, M. and P. Maak. 2000. Preliminary structural analyses of a sued fuel disposal container geometric alternativels. Ontario Power Generation, Nuclear Waste Management Division Report 06819-REP-01300-10012-R00.

Shoesmith, D.W., W. Lee, and D.S. Owen. 1981. Power Industry Res. 1, 253.

Shreir, L.L. 1976. Corrosion. 2nd edition, Newnes-Butterworths, London.

Simpson, J.P. 1989. Experiments on canister materials for Swiss high- level waste disposal projects, Part IV. National Cooperative for the Storage of Radioactive Waste Technical Report, NAGRA-NTB-89-19.

Simpson, J.P. and P.-H. Valloton. 1986. Experiments on container materials for Swiss high-level waste disposal projects, Part III. Nagra Technical Report 86-25

Smailos, E., W. Schwarzkopf, B. Fiehn and R. Köster. 1985. Corrosion behaviour of container materials in saliferous environments. Commission of European Communities Report, EUR-9570/1985.

Smart, N.R., D.J. Blackwood, and L.O. Werme. 2001: The anaerobic corrosion of carbon steel and cast iron in artificial groundwaters. SKB Technical Report TR-01-22.

Smart, N.R., D.J. Blackwood, and L.O. Werme. 2002. Anaerobic corrosion of carbon steel and cast iron in artificial groundwaters: Part 1 – electrochemical aspects. Corrosion 58, 547-559.

Stahl, D., J.K. McCoy, and R.D. McCright. 1995. Impact of thermal loading on waste package material performance. Mat. Res. Soc. Symp. Proc. 353, 671-678.

Stratmann, M. and J. Muller. 1994. The mechanism of the oxygen reduction on rust-covered metal substrates. Corrosion Science 36, 327-359.

Stroes-Gascoyne, S. and F. King. 2002. Microbially influenced corrosion issues in high-level nuclear waste repositories. Proc. CORROSION/2002 Research Topical Symposium, NACE International (Houston, TX).

Stroes-Gascoyne, S., C.J. Hamon, C. Kohle, and D.A. Dixon. 2006. The effects of dry density and porewater salinity on the physical and microbiological characteristics of highly compacted bentonite. Ontario Power Generation, Nuclear Waste Management Division Report 06819-REP-01200-10016.

Stroes-Gascoyne, S., C.J. Hamon, D.A. Dixon, C.L. Kohle, and P. Maak. 2007. The effects of dry density and porewater salinity on the physical and microbiological characteristics of compacted 100% bentonite. In Scientific Basis for Nuclear Waste Management XXX, (D.S. Dunn, C. Poinssot, B. Begg, Editors), Mat. Res. Soc. Symp. Proc. 985, Materials Research Society, (Warrendale, PA), in press.

Stumm, W. 1992. Chemistry of the Solid-water Interface, Wiley-Interscience, New York.

Szklarska-Smialowska, Z. 2005. Pitting and Crevice Corrosion. NACE International (Houston, TX).

Turnbull, A. 1993. Review of modelling of pit propagation kinetics. Br. Corros. J. 28, 297-308.

Turnbull, A. and A.T. May. 1987. Steady state electrochemical kinetics of BS 4360 50D structural steel in deaerated 3.5%NaCl solution of varying pH. Brit. Corrosion J. 22, 176-181.

Vago, E.R. and E.J. Calvo. 1992. Electrocatalysis of oxygen reduction at Fe_3O_4 oxide electrodes in alkaline solutions. J. Electroanal. Chem. 339, 41-67.

Wroblowa, H.S. and S.B. Qaderi. 1990. Mechanism and kinetics of oxygen reduction on steel. J. Electroanal. Chem. 279, 231-242.

Yokoyama, Y., H. Mitsui, R. Takahashi, A. Otsuki, H. Asaon, N. Taniguchi, and M. Yui. 2007. Corrosion behaviour of the weld zone of carbon steel overpack for HLW disposal – corrosion behaviour under the aerobic conditions at the early stage of the post-closure repository phase. Presentation at CORROSION/2007, Research-on-Progress Symposium (NACE International, Houston, TX).

You, D., N. Pebere and F. Dabosi. 1993. An investigation of the corrosion of pure iron by electrochemical techniques and *in situ* observations. Corrosion Science 34, 5-15.

Zecevic, S., D.M. Drazic and S. Gojkovic. 1991a. Oxygen reduction on iron –IV. The reduction of hydrogen peroxide as the intermediate in oxygen reduction reaction in alkaline solutions. Electrochimica Acta 36, 5-14.

Zecevic, S., D.M. Drazic and S. Gojkovic. 1991b. Oxygen reduction on iron –V. Processes in boric acid-borate buffer solutions in the 7.4-9.8 pH range. Corrosion Science 32, 563-576.

Zhang, J., J. Wang, and Y. Wang. 2005. Micro-droplets formation during the deliquescence of salt particles in atmosphere. Corrosion 61, 1167-1172.

Table 1: Summary of Corrosion Rate Predictions for C-steel Used Fuel Containers

Country	Host formation	Uniform corrosion	Localized corrosion	Environmentally assisted cracking	Other	Corrosion prediction
United Kingdom (Marsh et al. 1987)	Granite	10 $\mu m \cdot a^{-1}$ during anoxic period (>125 a*)	Max. pen. = $8.35t^{0.46}$ for period of passive conditions (125 a)	Stress relief to avoid SCC and post-weld heat treatment to soften HAZ to avoid H embrittlement	-	86 mm in 1000 a
United Kingdom (Marsh and Taylor 1988)	Granite	Aerobic period 1 mm Anaerobic period <10 $\mu m \cdot a^{-1}$ Additional 7 mm due to radiolysis	Max. pen. = $8.35t^{0.46}$ (based on EVA) calculated for entire period	SCC mitigated by stress relief heat treatment	Max. pen due to MIC = 13 mm, based on organic C limitation	231 mm in 1000 a
United Kingdom (Marsh and Taylor 1988)	Granite	216 $\mu m \cdot a^{-1}$ based on electrochemical active model, including effect of radiolysis	Max. pen. = $8.35t^{0.46}$ (based on EVA) calculated for entire period. Not additive to rate of uniform corrosion.	-	-	216 mm in 1000 a
United Kingdom (Marsh et al. 1989)	Marine sediments	Electrochemical model under active conditions, including radiolysis	None, O_2 supply insufficient to sustain passive conditions	-	-	33 mm in 1000 a
Japan (JNC 2000)	Not yet defined.	50 mm in 1000 a, based on electrochemical model	None, only active dissolution in compacted buffer.	No H embrittlement, sulphide stress cracking, or HIC based on threshold [H] arguments.	No MIC due to survivability in compacted buffer.	50 mm in 1000 a

*125 a = 125 years

….. continued

Table 1: Summary of Corrosion Rate Predictions for C-steel Used Fuel Containers (concluded).

Country	Host formation	Uniform corrosion	Localized corrosion	Environmentally assisted cracking	Other	Corrosion prediction
Japan (JNC 2000)	Not yet defined.	Aerobic period 0.3-1.8 mm depending on repository design, based on O_2 mass balance. 10 $\mu m \cdot a^{-1}$ during anoxic period.	Additional pit depth 4.1-10.0 mm during aerobic period depending on repository design. Pitting factor = 2, corresponding to additional 10 mm pit depth during anoxic period.	No H embrittlement, sulphide stress cracking, or HIC based on threshold [H] arguments.	MIC taken into account during anoxic period based on conversion of SO_4^{2-} to HS^-	24.6 mm, 30.7 mm, and 31.8 mm in 1000 a for in-room, in-borehole (hard rock) and in-borehole (soft rock), respectively.
Switzerland (Johnson and King 2003)	Crystalline, Opalinus Clay	<1 mm during aerobic phase, based on mass-balance. Corrosion rate 1 $\mu m \cdot a^{-1}$ during anoxic period. 0.02 $\mu m \cdot a^{-1}$ due to HS^- diffusion, including localized corrosion	Pitting corrosion during aerobic phase = 10 mm based on empirical pitting factor.	No SCC based on absence of cyclic loading and aggressive species. No H-related failures due to absorbed [H] below threshold concentration	No MIC based on absence of microbial activity in compacted bentonite.	~12 mm in 1000 a. ~21 mm in 10,000 a.
Canada (King 2005a)	Sedimentary rock	0.087 mm due to O_2 during aerobic phase. Corrosion rate of 0.1-1.0 $\mu m \cdot a^{-1}$ during anoxic period	Depth-dependent pitting factor	No SCC based on absence of cyclic loading and aggressive species. No H-related failures due to absorbed [H] below threshold concentration	MIC not included because of use of 100% bentonite in repository and assumption of no microbial activity in host rock	9-34 mm in 10,000 a 34-175 mm in 10^5 a depending on anoxic uniform corrosion rate